Australian Government
Department of Defence
Defence Science and
Technology Organisation

Environmental Durability Trial of Bonded Composite Repairs to Metallic Aircraft Structure

Andrew Rider, Ian Williams Ed Shum and Leo Mirabella

Air Vehicles Division
Platforms Sciences Laboratory

DSTO-TR-1685

ABSTRACT

An agreement between DSTO and the US Air Force Research Laboratory (AFRL) was established as a part of a larger Aging Aircraft Project Agreement (PA). As a part of this agreement a large experimental program was organised to examine the long-term environmental durability of bonded composite repairs to metallic aircraft structure. An important aspect of the program was to examine the reliability and performance of current or recently developed surface treatments for metallic surfaces being repaired in field situations. The program involved the production of over 100 metal skinned honeycomb beam samples that were each patched with boron composite doublers. The beam samples are now being cyclically loaded in four point bending rigs at the DSTO tropical test facility in Innisfail, northern Queensland. It was anticipated that cyclic loading of the beams would result in adhesive disbonding for samples where the surface treatments were known to be inferior on the basis of accelerated laboratory testing. The overall results were hoped to enable the durability of metal to adhesive bonds present in boron composite repairs to be assessed for conditions similar to those expected in aircraft operating environments. An additional outcome of the research was hoped to be the ability to correlate accelerated durability testing conducted in the laboratory with more realistic aging conditions expected in aircraft service.

Published by

DSTO Platforms Sciences Laboratory
506 Lorimer St
Fishermans Bend, Victoria 3207 Australia

Telephone: (03) 9626 7000
Fax: (03) 9626 7999

AR-013-333
February 2005

APPROVED FOR PUBLIC RELEASE

Environmental Durability Trial of Bonded Composite Repairs to Metallic Aircraft Structure

Executive Summary

Bonded composite repair of metallic structure has become a useful aircraft structural life extension solution over the last two decades. Repairs have been applied to aircraft worldwide and in the last decade, the United States Air Force (USAF) has used bonded repair technology to solve some difficult flight safety and fleet readiness problems.

In Australia, the Royal Australian Air Force (RAAF) has been using bonded technology in niche applications for over 20 years. One of the initial applications involved repair to the Mirage III fleet, whilst repairs to F-111 have been ongoing. DSTO and the RAAF also applied a patch to the F-111 lower wing skin in a region that contained a critical crack for the limit load condition.

The most extensive use of bonded composite repairs to metallic structure in the USAF was for the wing-cracking problem in the Lockheed C-141. Over one thousand patches were applied to cracked fuel weepholes in the aging Starlifter. For the C-141, the repair option was the most practical solution to ensure the flight safety of the fleet, whilst maintaining operational readiness. Although part replacement would have served to restore structural integrity to an original condition, the wing planks in question were complex, 33-foot-long, integrally stiffened, highly priced items. As such, no stockpile of parts existed, and Lockheed was incapable of producing the components in the volume and time required to prevent a significant impact on fleet availability.

Whilst there are obvious advantages in using bonded repairs, the technology does have disadvantages, which have limited the widespread application on aircraft fleets throughout the world. Bonded repairs typically are not preferred in applications where bolted repairs or component replacement are feasible. Commercial airline maintenance organisations rarely use bonded repairs due to risks and complications perceived by many practising engineers. The reliability of bonded repairs relies heavily on the skills of the technicians applying the repairs and the quality of the engineering systems the practitioners adhere to. Due to a limited number of isolated incidents in which bonded structure on aircraft have catastrophically failed, the technology is not yet considered to be mature. In contrast to the perceptions of commercial airline maintenance engineers, defence based applications of the technology have been very reliable. The implementation of quality management systems by the RAAF have produced durable and reliable repairs on a range of aircraft for a number of years.

Additionally, the long-term environmental durability of adhesively bonded structure cannot be easily predicted without supporting field evidence. Typically, certification can only be provided in initial construction, where quality control of the bonding procedures can be guaranteed within the confines of a factory environment. It is more difficult for bonded repairs carried out on aircraft structure in the field to be performed with similar environmental control and repairs, as such, are not given structural credit. Clearly, the ability to certify the environmental durability of bonded repairs will expand their application and will offer substantial cost benefits to aircraft maintenance. Research and development needs to focus on methods to improve and guarantee the reliability of the technology and, therefore, facilitate certification and consequent widespread usage.

An agreement between DSTO and the US Air Force Research Laboratory (AFRL) was established as a part of a larger Aging Aircraft Project Agreement (PA). As a part of this agreement a large experimental program was organised to examine the long-term durability of bonded composite repairs to metallic aircraft structure. An important aspect of the program was to examine the reliability and performance of current or recently developed surface treatments for metallic surfaces being repaired in field situations. The program involved the production of over 100 metal skinned honeycomb beam samples that were each patched with boron composite doublers. The beam samples are now being cyclically loaded in four point bending rigs at the DSTO tropical test facility in Innisfail, northern Queensland. It was anticipated that cyclic loading of the beams would result in adhesive disbonding for samples where the surface treatments were known to be inferior on the basis of accelerated laboratory testing. The overall results were hoped to enable the durability of metal to adhesive bonds present in boron composite repairs to be assessed for conditions similar to those expected in aircraft operating environments. An additional outcome of the research was hoped to be the ability to correlate accelerated durability testing conducted in the laboratory with more realistic ageing conditions expected in aircraft service.

The current report details the beam construction and patch lay-up, together with the details of the surface pretreatments applied to the metallic adherend and the loading conditions employed, as well as initial results from testing.

Authors

Andrew Rider
Air Vehicles Division

Andrew Rider joined Airframes and Engines Division at DSTO in 1988. He has a PhD in Physical Chemistry from the University of New South Wales and is currently employed as a Research Scientist with Air Vehicles Division. He is involved in research to support RAAF maintenance of bonded structure and application of composite repairs used on ADF aircraft.

Ian Williams
Maritime Platforms Division

Ian Williams is a senior professional working at DSTO's tropical test facility in Innisfail, northern Queensland. Ian has extensive experience in laboratory instrumentation and has been involved in a wide range of defence based projects examining the influence of tropical exposure on defence equipment and materials performance.

Ed Shum
Maritime Platforms Division

Ed Shum has been working as a professional officer for MPD at DSTO's Innisfail test facility for a number of years. Ed has experience in the set-up and ongoing maintenenace of long term environmental testing undertaken at the Innisfail facility.

Leo Mirabella
Air Vehicles Division

Leo Mirabella joined DSTO in 1984 as a Technical Officer. He graduated from Royal Melbourne Institute Technology in 1992 with a Bachelor of Aeronautical Engineering. He has extensive experience in structural testing of metal, composite materials, bonded and bolted joints. He currently works in the area of composite materials and bonded composite battle damage repair

---

Contents

1. Introduction

Bonded composite repair of metallic structure has become a useful aircraft structural life extension solution over the last two decades. Repairs have been applied to aircraft worldwide [1] and in the last decade, the United States Air Force (USAF) has used bonded repair technology to solve some difficult flight safety and fleet readiness problems.

In Australia, the Royal Australian Air Force (RAAF) has been using bonded technology in niche applications for over 20 years. One of the initial applications involved repair to the Mirage III fleet [2], whilst repairs to F-111 have been ongoing. DSTO and the RAAF also applied a patch to the F-111 lower wing skin in a region that contained a critical crack for the limit load condition [3].

The most extensive use of bonded composite repairs to metallic structure in the USAF was for the wing-cracking problem in the Lockheed C-141. Over one thousand patches were applied to cracked fuel weepholes in the aging Starlifter [4]. For the C-141, the repair option was the most practical solution to ensure the flight safety of the fleet, whilst maintaining operational readiness. Although part replacement would have served to restore structural integrity to an original condition, the wing planks in question were highly expensive components to replace. As such, no stockpile of parts existed, and Lockheed was incapable of producing the components in the volume and time required to prevent a significant impact on fleet availability.

Whilst there are obvious advantages in using bonded repairs, the technology does have disadvantages, which have limited its widespread application on aircraft fleets throughout the world. Bonded repairs typically are not preferred in applications where bolted repairs or component replacement are feasible. Commercial airline maintenance organisations rarely use bonded repairs due to risks and complications perceived by many practising engineers. The reliability of bonded repairs relies heavily on the skills of the technicians applying the repairs and the quality of the engineering systems the practitioners adhere to. Due to a limited number of isolated incidents in which bonded structure on aircraft has catastrophically failed, the technology is not yet considered to be mature. In contrast to the perceptions of commercial airline maintenance engineers defence-based applications of the technology have been very reliable. The implementation of quality management systems by the RAAF have produced durable and reliable repairs on a range of aircraft for a number of years.

Additionally, the long-term environmental durability of adhesively bonded structure cannot be easily predicted without supporting field evidence. Typically, certification can only be provided in initial construction, where quality control of the bonding procedures can be guaranteed within the confines of a factory environment. It is more difficult for bonded repairs carried out on aircraft structure in the field to be performed with similar environmental control and repairs, as such, are not given structural credit.

Clearly, the ability to certify the environmental durability of bonded repairs will expand their application and will offer substantial cost benefits to aircraft maintenance. Research and development needs to focus on methods to improve and guarantee the reliability of the technology and, therefore, facilitate certification and consequent widespread usage. DSTO and ASI are currently developing processes and systems which are designed at increasing the quality of bonding operations and officially recording the performance of field repairs to provide direct evidence for the highly reliable performance of bonded repairs performed by RAAF for more than 10 years.

An agreement between DSTO and the US Air Force Research Laboratory (AFRL) was established as a part of a larger Aging Aircraft Project Agreement (PA). As a part of this agreement a large experimental program was organised to examine the long-term durability of bonded composite repairs to metallic aircraft structure. An important aspect of the program was to examine the reliability and performance of current or recently developed surface treatments for metallic surfaces being repaired in field situations. The program involved the production of over 100 metal skinned honeycomb beam samples that were each patched with boron composite doublers. The beam samples are now being cyclically loaded in four point bending rigs at the DSTO tropical test facility in Innisfail, northern Queensland. It was anticipated that cyclic loading of the beams would result in adhesive disbonding for samples where the surface treatments were known to be inferior on the basis of accelerated laboratory testing. It was hoped that the overall results would enable the assessment of the durability of metal to adhesive bonds present in boron composite repairs for conditions similar to those expected in aircraft operating environments. An additional outcome of the research was hoped to be the ability to correlate accelerated durability testing conducted in the laboratory with more realistic ageing conditions expected in aircraft service.

Presented in this report are the details of the beam construction and patch lay-up, together with the details of the surface pretreatments applied to the metallic adherend and the loading conditions employed, as well as initial results from testing.

2. Test Variables

The primary test variables examined in the program include the surface treatment applied to the metallic adherend, including the effect of chromate primers, adhesive type, and patch taper angle.

2.1 Surface Treatment

The most crucial part of the bonded repair installation process is the surface preparation of the metal being patched. The success in Australia and the US of bonded repairs has relied on the development of robust Engineering Standards, underpinned by effective personnel training. The inability of any currently available NDI procedures to accurately determine the quality of an adhesive bond means the success of the technology relies on the skills of the technicians applying the repairs and the quality control of the engineering systems in place. Rigid quality control and effective personnel training are often seen as a restriction for the increased use of bonded repairs due to the associated cost and time burdens. However, the development of adhesive bonding into a mature and accepted technology cannot overlook these critical aspects. Once greater confidence in the technology is established, these perceived time and cost disadvantages would be easily outweighed by the range of substantial advantages bonded repairs offer in numerous applications.

2.1.1 Established Surface Treatments

DSTO and RAAF have typically employed a surface treatment known as the "Australian Silane Treatment" for a number of years in bonded composite repairs to metallic structure and metal to metal repairs in F-111 honeycomb panel maintenance [5]. The AFRL Materials Directorate carefully examined the process variables and determined that conditions employed by DSTO were, in general, optimal [6]. The grit-blast and silane process (GBS) involves degreasing the metallic surface, abrading to remove weakly adhered layers, followed by grit-blasting and application of an epoxy silane coupling agent, prior to bonding. The process is a convenient and durable treatment for on-aircraft repairs. The best factory treatment available for bonding to aluminium alloys is the phosphoric acid anodisation process (PAA) [7], which involves deoxidising the aluminium prior to anodisation in a 10% phosphoric acid solution at approximately 10V for 10-15 minutes. PAA cannot be used for repairs on in-service aircraft and two versions for in-field use have been developed, the phosphoric acid containment system, or PACS [8], and the phosphoric acid non-tank anodise, or PANTA [9]. DSTO and the RAAF successfully used PANTA on 180 repairs to Mirage III lower wing skins [10].

Regardless of the process, a good surface preparation can require between four and ten hours to complete, and at times, 14 hours or more may be required for the entire patch installation. In many cases, however, this is still considerably faster than implementing a comparable bolted repair. Increasing the speed of surface preparation without compromising quality is, however, a useful objective in increasing the usage of the technology, particularly in areas of secondary and tertiary structure.

The RAAF and USAF have adopted two slightly different versions of the GBS process in that the RAAF does not use primer during patch application. Chromated primers pose an increased health and safety risk to workers and application is by no means a fail-safe step, as the thickness of the primer layer is critical to its effectiveness. Once the primer layer exceeds prescribed thickness values, the adhesive joint strength can be reduced due to the formation of a brittle interfacial layer. Additionally, recent research [11] has indicated that the primer offers no obvious benefit in durability, as measured by the wedge test, when FM73 adhesive is co-cured at 80°C for 8 hours. This is typically the case for minimising thermal residual stresses in field repairs using boron composites. The research has shown that primered GBS systems perform slightly better in standard Boeing Wedge Test (BWT) and Long Crack Extension (LCE) experiments for the FM73 standard cure condition of 120°C [11]. Clearly, however, the BWT and LCE tests are conducted in a laboratory to provide accelerated aging, but cannot be used to estimate the true long-term durability of an adhesive joint in service. RAAF anecdotally report very few problems with repairs carried out at Amberly on F-111, mainly on the secondary and tertiary structure of metallic skinned honeycomb panels. Presently, a survey is underway in order to quantify these assertions, and it is hoped teardown of representative patches will provide direct evidence of the surface treatment success. In contrast, the USAF still allows the use of primer in repair installation, but health and safety concerns may soon restrict its use as it has in the RAAF. Clearly the program will provide valuable long-term performance data on the influence of primers on bonded repair durability.

2.1.2 New Surface Treatments

Beyond altering the traditional surface preparation processes to become more time friendly, other options include developing altogether new surface preparations. The Sol-Gel surface preparation was developed by Boeing under contract from the Materials Directorate of AFRL and is now sold commercially through AC Tech as the product AC-130 [12]. The Sol-Gel technology is based on the GBS process and uses the same epoxy-silane coupling agent. In addition to the epoxy-silane, a zirconium-based alkoxide is also used. The application of dilute zirconium alkoxide and epoxy-silane mixture in aqueous solution provides a thin inorganic zirconium oxide film incorporated with epoxy-silane. The zirconium reacts with the metallic surface to produce a covalent chemical bond and the epoxy-silane provides a reactive organic group for bonding to the epoxy adhesive. The possible improvement of the sol-gel process over the GBS process would rely on the increased hydrolytic stability of the zirconium bonding to the metal and epoxy-silane and adhesive, compared with the straight epoxy-silane bonds to the metal and adhesive. An obvious benefit of the sol-gel process providing a more chemically resistant adhesive bond would be an increase in the speed and a reduction in the complexity of application. Such advantages may facilitate removal of the difficult grit-blasting step. Similarly, a better chemical bond may imply increased robustness of the process and, therefore, increased tolerance in production.

2.1.3 Surface Treatment Issues Addressed by the Durability Trial

The primary objectives of the bonded repair durability trial are the correlation of long-term bond durability with the metallic surface treatment, relating the durability assessed in the trial with accelerated testing conducted in laboratories and assessing the performance of established factory and field based metallic surface treatments with the recently developed sol-gel process.

The established treatments considered in the trial are the PAA and GBS processes. The PAA process provides a benchmark for the trial, as it is the best factory treatment available, and is only ever used with a chromate based primer. The GBS treatment is the most widely used process employed by RAAF and is used with and without a chromate primer in the trial to represent the variability that exists in field repair applications. The trial may also provide an indication of the relative effect that a small improvement in durability, observed by use of the primer with the GBS treatment in the wedge and LCE test, has on service life.

The GBS process has also been varied to simulate varying degrees of quality that may be possible in real life application (Table A1, Appendix A). These variations include extreme cases where the grit-blasting and silane treatment may have been overlooked (designated the Scotchbrite abrasion treatment (SB)), the epoxy-silane application is missing (designated the grit-blast treatment (GB)), the silane is applied without the grit-blasting (designated the Scotchbrite abrasion and silane treatment (SBS)) and the epoxy-silane solution is only 50% of the required concentration (designated the bad silane treatment (BS)). The benefit of these variations is to provide a realistic assessment of varying lapses in quality control of the GBS treatment on service life durability. Additionally, because these variations provide a wide spectrum of wedge test and LCE performance, the trial data will serve as a "calibration curve" for relating accelerated testing to service life performance.

The new sol-gel treatment is also examined in terms of its sensitivity to each of the processing steps to overall bond durability performance. Sol-gel is applied to the metallic surface with and without primer and with and without grit-blasting. The variations in treatment, thereby, provide the ability to relate performance directly with the GBS process and ascertain the sensitivity of the process to quality control.

2.2 Adhesive Evaluation

Two different adhesives have been selected for use in the durability trial, namely: FM-73 and FM 300-2. FM-73 has been used extensively in bonded repair applications undertaken by DSTO [1] and was used in the Starlifter program mentioned previously [4]. Whilst the recommended cure of 120°C (248 °F) has been used in this program, a cure at 80°C (176 °F) is typically used in field repairs. The increased cure temperature used in the trial will provide a valuable assessment of the influence of residual thermal stresses on durability, particularly for high and low peel stress patching configurations, referred to below. FM-73 is adequate for repairs to structures not expected to see temperatures above 80°C. For applications that stand to see slightly higher temperatures (up to 100 °C), FM 300-2 is an alternative. Thus FM 300-2 could be used on repairs to supersonic aircraft where aerodynamic heating becomes an issue. The choice of two adhesives allows the durability trial to evaluate repair configurations for adhesives that would typically be employed for the operational temperature envelopes of most defence aircraft.

2.3 Patch Design Variations

Another goal of the durability trial is to investigate the impact of different patch designs on the above combinations of surface preparations and adhesives. The final patch designs are straightforward, as shown in Figures 1 and 2. The two designs are very similar, with the only difference being in the stacking sequence of boron fibre plies and the taper ratio. The differences in taper ratio cause the two patches to be of slightly different lengths. The key is that one patch design will induce higher (undesirable) peel stresses at the tip of the patch. The other design, naturally, will be of a more optimum configuration and seek to minimise the peel stresses at the patch termination.

Using a combination of basic patch design guidelines and physical constraints caused by the specimen and load frame combination, the general design parameters for the low-peel patches are as follows:

- Extensional stiffness: 1.1
- Taper step-off rate: 25:1—3 mm (0.118 inch) steps
- Total length: 152 mm (6 inch)—limited to 190mm maximum by the load fixture
- Patch shape: Rectangular
- Width: 40 mm (1.575 inch)—same as specimen width
- Adhesive plies: 1
- Stacking sequence: Inverse wedding cake
- Thickness: 4 plies (4 x 0.0052”=0.0208”)

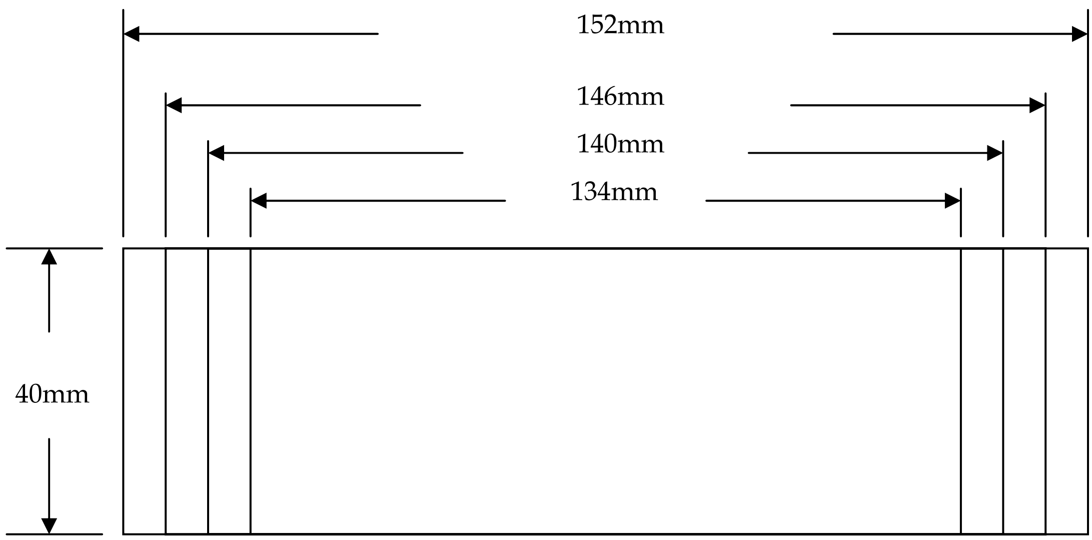

Figure 1 *Low-peel-stress patch design.*

The second patch design serves to maximise load attraction into the composite and minimise the repaired stress intensity (if damage were present). A higher peel stress at the patch tips should also result. The key design parameters for this patch follow:

- Extensional stiffness: 1.1
- Taper step-off rate: 12.5:1—1.5mm (0.059 inch) steps
- Total length: 133mm (5.25 inches)
- Patch shape: Rectangular
- Width: 40mm (1.575 inch)—same as specimen width
- Adhesive plies: 1
- Stacking sequence: Wedding cake
- Thickness: 4 plies (4 x 0.0052″=0.0208″)

Again, the only differences between the two patch designs are the taper step-off rate, the length (a direct result of the tapering), and the stacking sequence of the boron fibre plies. The inverse wedding cake sequence as used on the low-peel stress specimens is traditional for on-aircraft repair. In this way, all plies have at least some portion in contact with the metal, and the largest ply on top provides some protection against accidental or environmental damage to the plies beneath. For the high-peel configuration, however, it will be necessary to use a wedding cake sequence, as the taper ratio is too severe to use an inverse lay-up with the stiff boron fibre.

The patch configuration with the higher patch-tip strains should be more sensitive to the harsh environmental conditions and, thus, be at higher risk of failure. While it is generally not sought to have high patch tip adhesive strains, certain design constraints may restrict the taper step-off rate. For instance, geometric constraints of the repaired part may force the length of the patch taper to be less than optimum. The increased peel strains expected for the patch detailed in Figure 2 will provide a more demanding test of the durability of the various surface treatments examined and when combined with the increased residual stresses created by the 120°C cure used for the FM-73 specimens, will provide a good range of adhesive strain conditions for the trial.

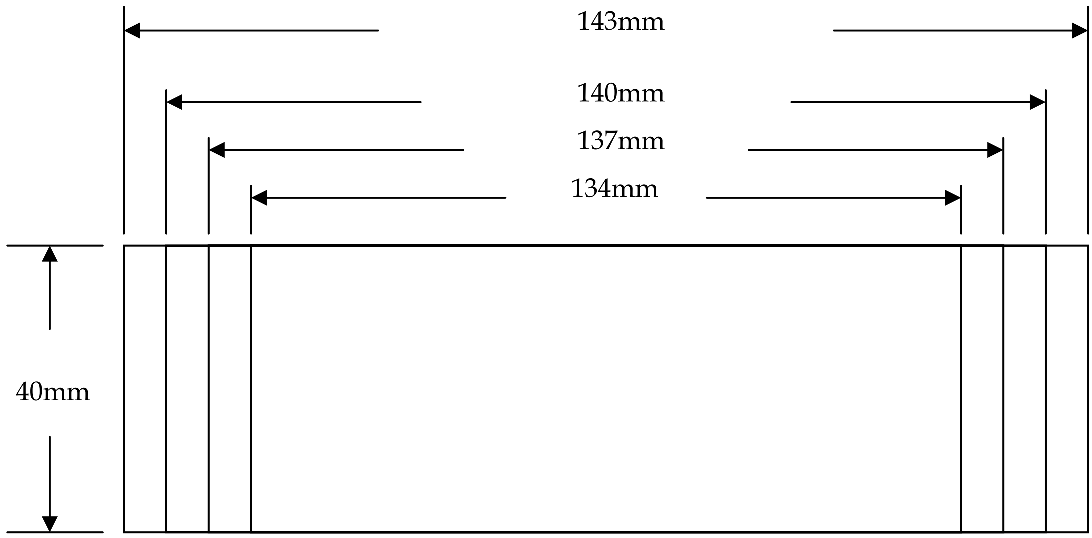

Figure 2 *High-peel-stress patch design.*

3. Test Matrix

The test matrix is provided in Appendix A, Table A2. The test facility at DSTO-Innisfail has 9 load frames (Figure 3), each with a capacity of 12 specimens (Figure 4), enabling 108 beams to be tested. The beams with the PAA treatment are all primed, include high and low peel stress patches, FM-73 and FM300-2 adhesive and have not been grit-blasted. The sol-gel treated beams are primed or unprimed, grit-blasted or not grit-blasted and have the patch and adhesive variations. The standard GBS treatments are varied by being primed or unprimed and also have the patch and adhesive variations. The off-optimum GBS treatments were added to the test matrix in the final stages and only examine the FM-73 in the low and high peel patch configurations. Each configuration is tested in triplicate to enable consistency in the testing to be established.

In the testing, the possibility of a block effect exists because several specimens are being tested in one load fixture. Differences in the fixtures might cause a different effect that is unrelated to the factors the test is designed to investigate. The only way to determine if these effects are significant is to insure triplicate samples are placed in different rigs and with different orientations. The position of each beam and its orientation is detailed in Appendix B, Table B1.

The Innisfail facility has the ability to monitor 80 strain gauge loads simultaneously during the fatigue loading. The positions of each strain gauge on the selected specimens are detailed in Appendix C.

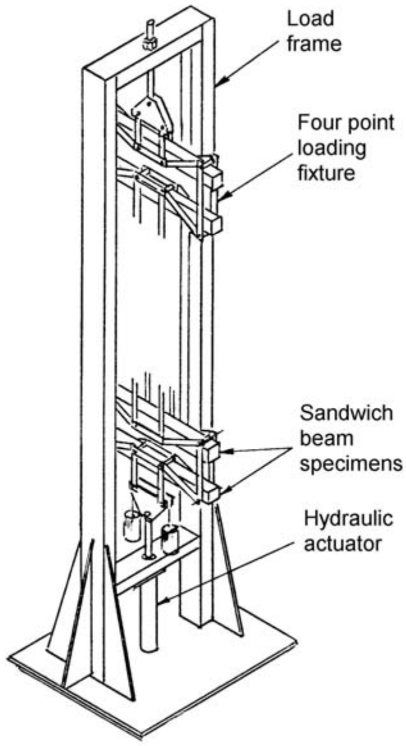

Figure 3 Loading rig at DSTO-Innisfail facility [13]

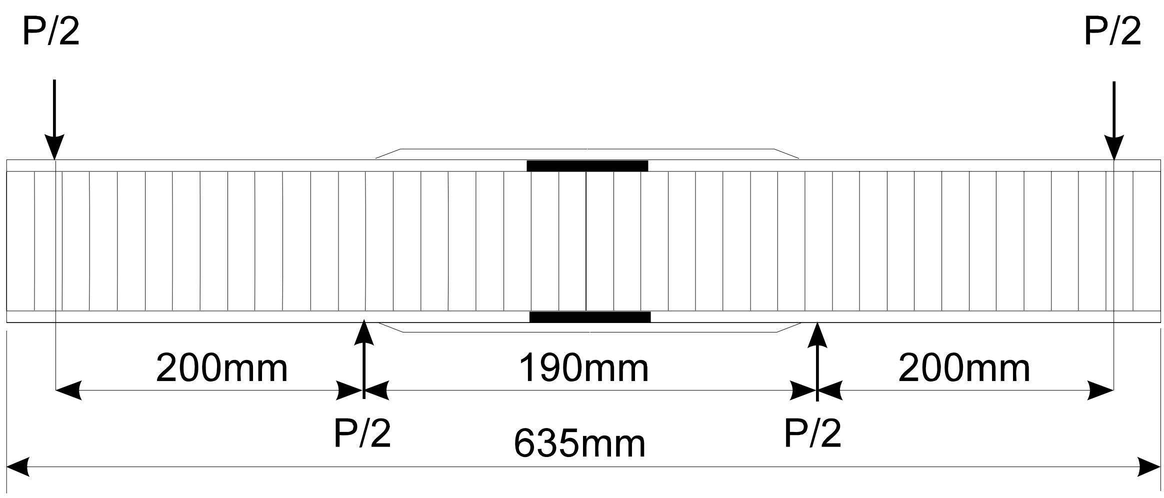

Figure 4 General specimen dimensions and load arrangement. The Aluminium face sheets are 40 mm wide and 1.27 mm (0.050 inch) thick [13].

4. Experimental Details

The DSTO facility in Innisfail, Queensland occupies land adjacent to a rainforest in one of the wettest places in Australia. On average, Innisfail receives four metres (157 inches) of rain per year, and has an average relative humidity of 83%. The average daily temperature is 24°C (75°F) with maximums occasionally reaching 40°C (104°F). Due to the nature of the environment, significant demands will be placed on the bonded joints, but also importantly on the testing equipment and facilities. During the set-up phase of this trial significant time and effort was devoted to overhauling the pump, hydraulics, wiring systems, load cells and dataloggers. Over 10 years of humid exposure had taken its toll on numerous items and during the course of the trial it would be expected further maintenance and overhaul will be needed. Additionally, obsolete data-logging systems will require replacement at some stage during the trial.

4.1 Specimen Fabrication

AFRL manufactured all the specimens used in this research program. Materials included aluminium face sheets and honeycomb core for the beams themselves and boron fibre and adhesive for the patches.

To build the basic beam, the bonding shop at the USAF Warner Robins Air Logistics Centre, (WR-ALC) used Cytec FM-300-2 to bond large sheets of aluminium honeycomb 5052 H-191 core (cell 1/8″, gage 0.002, 8.1 pcf) from Hexcel to face sheets of 1.27 mm (0.050 inch) Alclad 2024-T3 aluminium. Before bonding, the large aluminium sheets were PAA treated in the process line at WR-ALC [7]. Due to initial panel lay-up, the majority of beams had to be cut with the honeycomb core running perpendicular to the length direction, which unfortunately doesn't provide optimum stiffness. Details of the panel cutting are provided in Figure 5. Using the two panels of PAA treated and BR-127 primed honeycomb, 140 beams of fixed length were cut. Fifty-eight beam specimens aligned perpendicular to the ribbon direction were cut from each panel. Twelve beam specimens aligned with the ribbon direction were also cut from each panel. The tolerance on the beam width was +/- 0.020″. Each beam cut perpendicular to the ribbon direction (or width direction) was etched with an ID number, starting with #1 and continuing through #116. The ID number corresponded to the run order number in Appendix A Table A2. Beams numbered from 109-114 were used for the calibration of the strain gauge loads, detailed in Appendix D. The remaining samples with the core running in the length direction were numbered and treated as detailed in Appendix A Table A3. These samples may be tested using accelerated laboratory procedures or tested at Innisfail should funding opportunities arise.

Boron-epoxy patches were laid up as detailed in Figure 1 and 2 using Boron-epoxy Prepreg Tape-5521/4 with nylon release plies on either side during autoclave cure at 120°C (250°F) and 50psi for 60 minutes. Before the cured patches were bonded to the pretreated metal surface of the honeycomb beams, the peel plies were removed and the bonding surface was solvent cleaned with methyl ethyl ketone (MEK), water-break free tested with distilled water, dried 60 minutes at 110°C (230°F) and grit-blasted lightly to produce a matte finish.

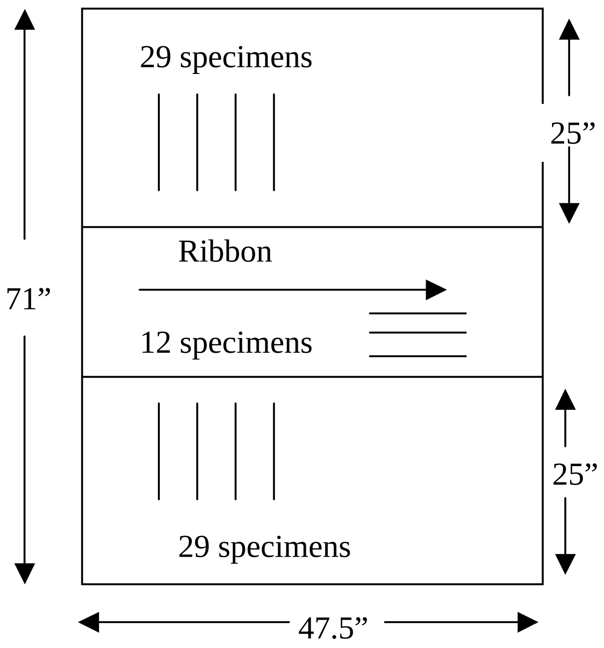

Figure 5

Figure 5 Panel cutting plan for the 2 panels produced for the beam manufacturing

Surface preparation of the aluminium skins, for the samples that were not to be bonded to the PAA and primed surfaces, involved abrasion using 3M Scotchbrite 8447, with MEK solvent to remove the existing PAA and primer layer. There was no direct intention to remove the clad layer from the aluminium surface, although additional examination of the beams after the trial is completed will be needed to verify the final state of the aluminium surface. The abraded surface was then solvent cleaned by unidirectional wiping of MEK soaked lint and lanoline free disposable cloths. Abrasion and wiping was then repeated replacing the MEK with distilled water. Cleaning was considered sufficient if a single pass of the tissue did not transfer contaminant from the surface. The surface was then water-break tested and dried at 110°C (230°F) for 5 minutes. In the case of the silane treated surfaces, epoxy silane (γ-glycidoxypropyltrimethoxy silane) was prehydrolysed for at least 1 hour in a 1 % solution of distilled water. After removal from the silane solution the surface was dried at 110°C (230°F) for 60 minutes. If BR-127 primer was applied, it was dried at room temperature for 30 minutes followed by oven dry at 121°C(250°F) for 30 minute, prior to bonding.

Table A1 provides details of the epoxy-silane pre-treatment samples where critical processing steps were removed from that detailed above. In the case of the sol-gel or

AC-130 treatment, Table 1 provides details of the process variations. All treatments were performed for both adhesives, both patch configurations..

Table 1 Beams with AC-130 (Sol-Gel) Surface Treatments

Surface treatment	Details	Primer
No grit-blast	Abrade with scotchbrite and MEK, followed by solvent wipe with tissues and MEK, paint with AC-130 solution, 10 minutes and dry at 110^{o}C	Yes
		No
Grit-blast	Abrade with scotchbrite and MEK, followed by solvent wipe with tissues and MEK, followed by grit-blast with 50mm alumina, paint with AC-130 solution, 10 minutes and dry at 110^{o}C	Yes
		No

AC-130 is available from AC-Tech[1] and is a surface treatment developed under contract by Boeing for adhesive bonding and is reported to be adaptable to a wide range of metals. The formulation is detailed in Table 2. The procedure for grit-blasting prior to AC-130 treatment application is detailed below:

Table 2 Composition of AC-130 from AC Tech

Material	Volume (mL)	Mass (g)
Glacial Acetic Acid	0.43	0.412
Zirconium (IV) Propoxide (70wt%)	0.97	1.03
γ-glycidoxypropyltrimethoxysilane (γ-GPS)	1.93	2.09
Distilled Water	96.67	96.67

1) solvent wiping: single wiping of the aluminium surface used methyl ethyl ketone (MEK) soaked lanoline and lint free tissues. A fresh tissue is used after each pass. Single wiping is conducted along the grain direction and at 90^0 relative to the grain until no observable debris or staining of the tissue can be observed,
2) Scotchbrite® abrasion with MEK: following solvent wiping the surface is abraded with Scotchbrite pad soaked in MEK along the grain direction and at 90^0 relative to the grain until a uniform surface appearance is observed. Single

[1] Advanced Chemistry&Technoogy 7341 Anaconda Avenue, Garden Grove, California 92841 phone 714 373-2837 fax 714 373-1913

wiping of the aluminium surface then uses MEK soaked lanoline and lint free tissues. A fresh tissue is used after each pass. Wiping is conducted in the direction of the abrasion until no presence of debris or staining of the tissue can be observed.

3) Grit-blasting: uniform grit-blasting of the surface employs 50 μm alumina grit and dry nitrogen propellant with a pressure of 450kPa and a working distance of 15 to 20cm
4) AC-130 treatment: the mixture detailed in Table 2 is mixed and allowed to sit for several hours prior to commencing the surface pre-treatment steps listed above. The grit-blasted aluminium surface is "immersed" in the AC-130 solution for 15 minutes by applying the solution regularly to the aluminium surface with a clean paint brush.
5) The AC-130 solution should be used within 8 hours of production. The aluminium surface is dried by forced removal of the solution from the surface with pressurised air. "Cross-linking" of the zirconate-silane film is then performed at 110^{o}C (230^{o}F) for 1 hour for optimal performance

The boron-epoxy patches fabricated above were bonded to the beams using FM-73 and FM-300-2K. FM-73 with a 0.085psf and knit carrier was cured 60 minutes at 120^{0}C (250^{0}F) using a ramp rate of 3^{0}C (6^{0}F) per minute and a vacuum pressure of 20 inches of mercury initially before commencing the heating. The pressure was reduced to 10 inches of mercury when the temperature reached 80^{0}C(176^{0}F). FM-300-2K with a 0.08 psf and a knit carrier was cured 90 minutes at 120^{0}C (250^{0}F) using a ramp rate of 3^{0}C (6^{0}F) per minute and a vacuum pressure of 20 inches of mercury initially before commencing the heating. The pressure was reduced to 10 inches of mercury when the temperature reached 80^{0}C (176^{0}F).

4.2 Specimen Loading

4.2.1 Fatigue Durability of Honeycomb Beams

Specimen loading was determined initially by establishing the maximum permissible load that the beams could withstand in fatigue for the duration of the trial. The properties and dimensions of the materials used in the beams are detailed in Table 3. Definitions of the terms used in the calculation of the fatigue properties of the honeycomb are detailed in Table 4.

Table 3 Beam material dimensions and properties

<table>
<tr><th></th><th>Width</th><th>Thickness</th><th>Length</th><th>Materials</th><th colspan="2">Mechanical Properties</th></tr>
<tr><td rowspan="3">Core</td><td rowspan="3">1.575″ (40mm)</td><td rowspan="3">1″ (25.4mm)</td><td rowspan="3">25″ (635mm)</td><td rowspan="3">CR3, 8.1pcf, 1/8″ cell, 1″ thick, 5052 alloy, 0.002 gage</td><td colspan="2">Plate Shear</td></tr>
<tr><td>L</td><td>W</td></tr>
<tr><td>800psi (average) 670psi (minimum</td><td>530psi (average) 400psi (minimum)</td></tr>
<tr><td rowspan="2">Skin</td><td rowspan="2">1.575″ (40mm)</td><td rowspan="2">0.05″ (1.27mm)</td><td rowspan="2">25″ (635mm)</td><td rowspan="2">Al-2024T3-</td><td colspan="2">Youngs Modulus</td></tr>
<tr><td colspan="2">72.4GPa</td></tr>
<tr><td rowspan="2">Boron-Epoxy</td><td rowspan="2">1.575″ (40mm)</td><td rowspan="2">0.13/ply</td><td rowspan="2">152/133 mm</td><td rowspan="2">5521/4</td><td>Longitudinal Modulus (GPa)</td><td>Ultimate Longitudinal Strain</td></tr>
<tr><td>207</td><td>0.006550</td></tr>
</table>

Table 4 Definitions of the terms and symbols used in the calculation of fatigue properties of the honeycomb beams used in the durability trial.

Symbol	Definitions [14]
τ_{limit}	honeycomb beam core shear stress in fatigue loading, psi
τ_{ult}	honeycomb beam ultimate core shear stress allowable, psi
τ_s	honeycomb beam ultimate core shear stress measured from plate shear test, psi (minimum strength quoted from Hexcel corporation in L direction [15])
P	applied load, lbF (4.448N)
W	beam width, in.
H	beam height or thickness, in. (core thickness + skin thickness)
K_θ	fatigue modification factor to allow for honeycomb core direction in beam
K_{config}	fatigue modification factor to allow for temperature, core density, face sheet thickness, core height, load span

Fatigue life assessment of the honeycomb core in 4 point bending was determined from reference [14] using equation (1),

$$\tau_{ult} = \tau_s . K_\theta . K_{config} \qquad (1)$$

where:

τ_s is 670psi, K_θ is 0.8, K_{config} is 0.95 (K_{config} was extrapolated from Figure 8, reference 1, pcf[2] 2.3 0.829, pcf 3.1 0.881, pcf 5.3 0.976.)

therefore:

$$\tau_{ult} = 510\text{psi}$$

Given the duration of durability trial is expected to be 5 years and the fatigue loading occurs at 0.013Hz and R=0, then [13]:

Number of Cycles required (N): (5y x 365d x 24h x 60m x 60s)/76.9=2,0498,840

From Figure 6 (reference 14):

$$\tau_{limit} / [\tau_s . K_\theta . K_{config}] = 1.0158\text{-}0.076531\log(N)$$

$$\tau_{limit} / \tau_{ult} = 0.456$$

$$\tau_{limit} = 0.456 \times 510 = 233\text{psi}$$

Therefore:

$$\tau_{limit} = P/[W \times H]$$
$$= P/[1.575 \times 1.1]$$

$$P = W \times H \times \tau_{limit}$$
$$P = 233 \times 1.575 \times 1.1$$
$$= 404\text{lbF} = \underline{\mathbf{1800N}}$$

[2] pcf=pounds per cubic foot

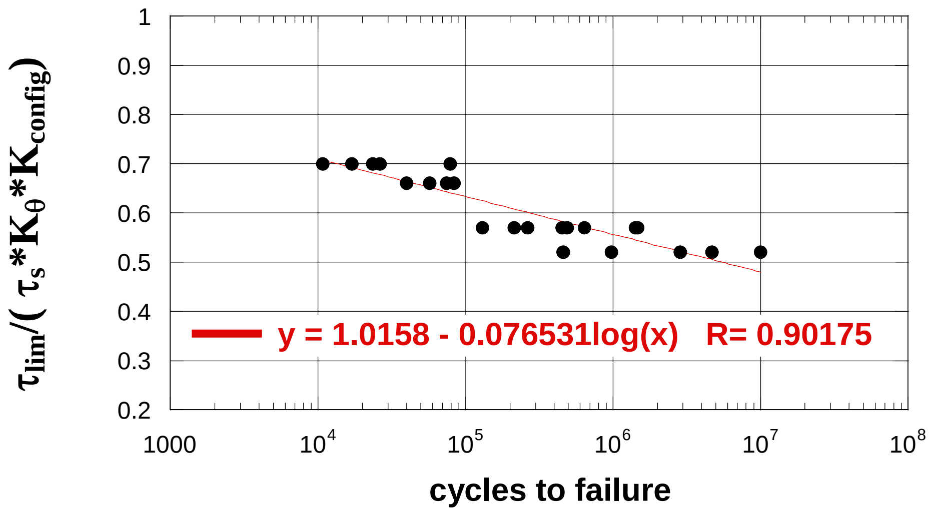

Figure 6 Cycles to failure for honeycomb beams manufactured from 3.1 pcf CRIII Hexcel core in width direction orientation from Ref 14 for R= -1

4.2.2 Static Stresses in the Boron Composite Patches

Appendix E: and Appendix F: detail the calculations used to determine the stresses in the honeycomb metallic skins both underneath and at the end of the patch as well as the strain level in the adhesive. The method used the formulae and processes detailed in AAP7021.016-1, Chapter 6, Appendix 2, Annexe C, for Single Sided Supported Repairs, pages 6C2-1 to 6C2-15. Briefly, the maximum fatigue load determined in section 4.2.1, was used to back-calculate the far-field stress in the aluminium skin and the equivalent stress in the adhesive, assuming all load is transferred through the patch. Beam loading in 4 point bending was determined from ASTM C-393. *Table 5* indicates the adhesive and skin stresses for the patched beams loaded at 1800N

Table 5 Summary of the adhesive and skin stresses for patched aluminium honeycomb beams load at 1800N in four point bending.

Adhesive	Elastic Shear Strain Limit (γ_e)	Max. shear strain (γ_{adh})	Stress Under the Patch (Skin) σ_{ups} (psi)	Stress at End of the Patch (Skin) σ_{eps} (psi)	Far-Field Stress (Skin) σ_s (psi)	4 Point Bending Load (N)
FM-73	0.102	0.085	1.325×10^4	2.901×10^4	1.536×10^4	1.808×10^3
FM-300-2K	0.0957	0.064	1.401×10^4	3.066×10^4	1.554×10^4	1.829×10^3

Appendix D: (Table D2) indicates the strains measured at room temperature and 80°C for the FM73 bonded patches in the 2 configurations.

4.2.3 Strain Monitoring of the Beams During Trial

Strains in the patches on the compression and tension sides are being logged from locations indicated in Figure C1 during the long term trial. Loads are also being monitored concurrently with the strain readings. The voltages from the strain gauges and load cells are logged with a Hewlett Packard 3497A Data Acquisition unit housed in an air conditioned laboratory. In order to allow for variations in strain with temperature due to thermal coefficient of expansion mismatch of the gauge and the patch, the compliance is monitored i.e. the load divided by the strain. During the loading cycle the first 21 voltage readings of load and strain are taken between 0N and approximately 1600N. This is done as the initial loading provides the linear portion of the load-strain curve. The measurements are repeated and the compliance of the patch is calculated and compared with the initial condition. Figure 7 indicates the results for Rig number 5 from December 03 to June 04. It can be seen that 4T1 and 4T2 fail in the early stages of the trial (Refer Appendix B:), referring to Scotchbrite only treatment and FM-73 with a high peel patch. At this stage NDI measurements of the remaining specimens which have the Scotchbrite only treatment, that did not contain strain gauges, have not been performed.

The procedure of calculating the strains from the logged voltages involves initially providing a zero load correction to the strain voltage reading. Zero strain voltage readings for the WA-03-125BT-120 Micro-Measurement gauges were taken with the beams in the ladder rigs disconnected from the hydraulic ram. This provides a reasonable approximation of a zero load condition, although beams will be bearing the weight of other beams and the rig. The strain voltage in the zero and loaded condition then needs to be normalised for the excitation voltage used (equation 1):

$$V_r = \frac{\left(V_{o(strained)}\right)}{V_{ex(strained)}} - \frac{\left(V_{o(unstrained)}\right)}{V_{ex(unstrained)}} \tag{1}$$

where V_r is corrected strain output voltage

$V_{o(strained)}$ is the strain output voltage during loading

$V_{o(unstrained)}$ is the strain output voltage at zero load

$V_{ex(strained)}$ is the strain excitation voltage at during loading

$V_{ex(unstrained)}$ is the strain excitation voltage at zero load

Table 6 indicates the excitation and strain voltages for strain gauges in the "zero" load condition. Output strain (ε) is then determined for quarter bridge circuit according to equation 2:

$$\varepsilon = \frac{-4V_r}{GF(1+2.V_r)} \qquad (2)$$

where GF is the gauge factor for the WA-03-125BT-120 Micro-Measurement gauges and was equal to 2.05. Correction for lead wire resistance was ignored as the effect on strain reading was insignificant relative to the measured strain values.

Table 6 Excitation and strain voltages for strain gauges in the "zero" load condition

Rig	1	2	3	4	5	Excitation
1A	-0.001111	-0.003065	-0.004225	-0.002399	-0.004953	5.0103
1B	-0.005624	-0.002544	-0.003315	-0.002893	-0.004653	5.0083
2A	-0.006220	0.012968	-0.003411	-0.002375	-0.004097	5.0093
2B	0.008219	-0.002314	-0.003079	-0.002211	-0.001391	5.0009
3A	-0.002406	-0.003031	-0.002460	-0.002972	-0.002942	5.0114
3B	0.003616	-0.002404	-0.004754	-0.003629	-0.005609	5.0057
4A	-0.001546	-0.003217	-0.001752	-0.003291	-0.004808	4.9951
4B	-0.004946	-0.002111	-0.002056	-0.002539	0.000354	4.9897
5A	-0.002070	-0.003704	-0.004101	-0.001277	-0.002744	4.9845
5B	-0.003658	-0.002488	-0.002195	-0.002088	-0.003251	4.9933
6A	-0.003207	-0.002688	-0.003375	-0.003246	-0.002708	4.9814
6B	-0.005449	-0.002121	-0.002469	-0.003239	-0.001506	4.9815
7A	-0.001348	-0.003151	-0.004183	-0.002902	-0.004060	4.9896
7B	-0.002710	-0.003512	-0.002363	-0.003141	-0.002360	4.9850
8A	-0.003761	-0.003626	-0.005695	-0.005088	-0.004056	4.9808
8B	-0.003746	-0.004274	-0.001669	-0.004890	-0.003112	4.9786

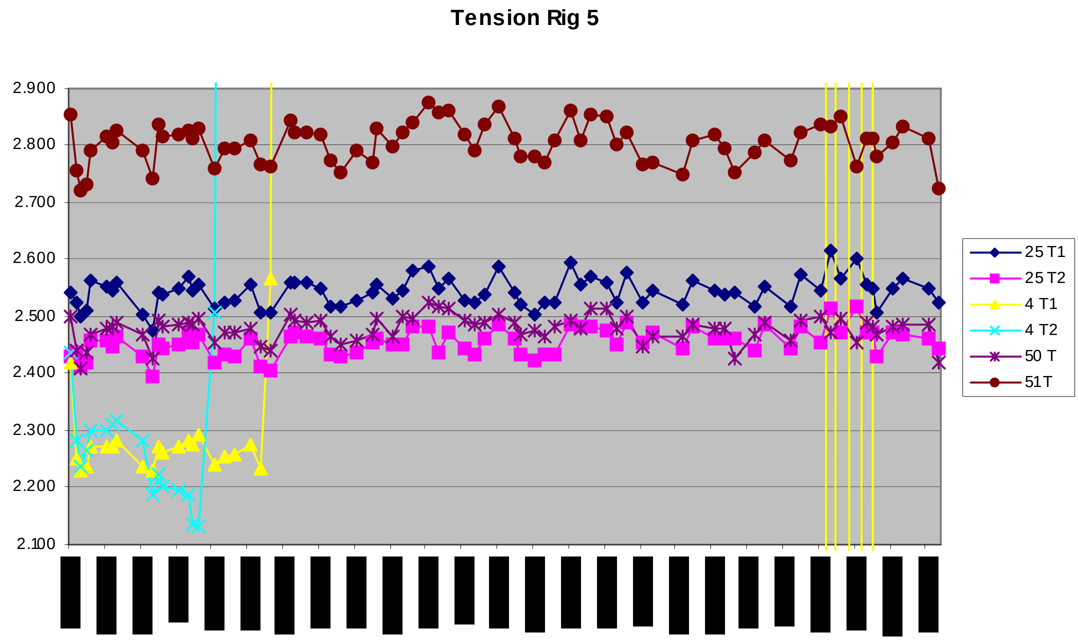

Figure 7 Load/Strain slope for Rig 5 beams from December '03 to June '04.

Load calibration was performed by manually applying calibrated weights to the load cells and recording voltage. A plot of load versus voltage enabled an average gradient and intercept to be determined for each load cell. Loads up to 186.37kg were applied and the slopes for each cell are provided in Table 7.

Table 7 Slope and intercept calculated for each of the 9 load cells used in the durability trial determined by measuring voltage as a function of load.

Rig #	Intercept	Slope
1	-1.613320	-19553.349822
2	0.448541	-20392.794944
3	-2.067262	-19751.158316
4	1.571375	20527.394710
5	-0.389074	-20136.254989
6	0.212409	-20008.455317
7	-2.588712	-19688.786729
8	2.029994	-19918.356254
9	-1.754614	23398.896418

Load (P) in Newtons was then calculated from the recorded output voltage, V_o, using equation 3:

$$P = ((V_o \times Slope) + intercept) \times 9.80665 \qquad (3)$$

A typical scan of the loads and strains for Rig 1, strain gauge 3 and the calculated slope is provided in Table 8.

Table 9 indicates the details of the strain gauge failures from December 2003 to November 2004. The Scotchbrite abrade samples failed rapidly, as expected, based on accelerated environmental resistance tests on similar treatments performed using the wedge test [16]. Strangely, the Scotchbrite abraded sample number 4, with the high peel patch, failed on the compression loaded side before the tension loaded side. The Scotchbrite abraded sample number 97, with the low peel patch, failed at similar times on the compression and tension sides and before the tension gauges on sample 4. The failures have been confirmed using tap testing. The remaining two samples appear to indicate strain gauge failure rather than disbonding.

Table 8 Typical output and calculated values for a load-strain scan of the rigs

Rig	1				
Date	12-15-2003				
Start time	11:46:23				
Load Cell Excitation (V)	10.0003				
Vo (unstrained)	-0.004225				
Vex (unstrained)	5.0103				
Vex(strained)	5.0088				
Load 3 (V)	**Load 3 (N)**	**Strain Gauge 3 (V)**	**Vr**	**Strain Gauge 3 (μE)**	**Load/strain**
-0.007881	1495.38301	-0.005645	-0.000283754	553.979895	2.699345271
-0.007942	1507.079934	-0.00565	-0.000284752	555.929903	2.710917196
-0.007999	1518.009847	-0.00566	-0.000286748	559.8299422	2.7115553
-0.008052	1528.172748	-0.005676	-0.000289943	566.0700699	2.699617644
-0.008103	1537.952144	-0.005688	-0.000292338	570.750218	2.69461508
-0.008149	1546.772776	-0.005698	-0.000294335	574.6503757	2.691676263
-0.00819	1554.634643	-0.005702	-0.000295134	576.2104475	2.698032723
-0.008232	1562.688263	-0.005709	-0.000296531	578.9405851	2.699220443
-0.00827	1569.974871	-0.005718	-0.000298328	582.4507846	2.69546357
-0.008305	1576.686221	-0.005719	-0.000298528	582.8408083	2.705174722
-0.008336	1582.63056	-0.005727	-0.000300125	585.9610092	2.700914455
-0.008369	1588.958404	-0.005741	-0.00030292	591.4214089	2.686677182
-0.0084	1594.902743	-0.00574	-0.00030272	591.0313783	2.69850773
-0.008426	1599.888317	-0.005747	-0.000304118	593.7615989	2.694496108
-0.008453	1605.065644	-0.005752	-0.000305116	595.7117658	2.694366196
-0.008475	1609.284207	-0.005758	-0.000306314	598.0519763	2.690876832
-0.008498	1613.694523	-0.005761	-0.000306913	599.2220858	2.692982387
-0.008522	1618.296592	-0.005764	-0.000307512	600.3921981	2.695399102
-0.008543	1622.323402	-0.005767	-0.000308111	601.5623132	2.696850128
-0.008563	1626.158459	-0.005779	-0.000310506	606.2428016	2.68235508
-0.008583	1629.993516	-0.005779	-0.000310506	606.2428016	2.688681023
-0.008603	1633.828573	-0.005782	-0.000311105	607.4129307	2.689815265
				Average	2.696251805

Table 9 Indications of disbonding from strain gauge readings from 15/12/03 to 8/11/04

Gauge/Specimen No.	Details	Gauge Failure Date	Cycles Completed	Comments
4C	SB, NBR, NGB, H, 7	15/12/03	25	Almost instantaneous failure of Scotchbrite abraded sample with high peel patch on compression side
97T	SB, NBR, NGB, L, 7	31/12/03	8883	Very rapid failure of Scotchbrite abraded sample with low peel patch on compression and tension side
97C		31/12/03	8883	
4T2	SB, NBR, NGB, H, 7	9/1/04	26493	Failure of Scotchbrite abraded sample with high peel patch on tension side
4T1		21/1/04	37400	
51C	G, NBR, NGB, H, 7	12/2/04	60334	Most likely failure of gauge
18T2	G, NBR, GB, H, 3	5/4/04	117039	Most likely failure of gauge

5. Summary

The current report details the motivation and mechanisms for examining the durability of a range of surface treatments relevant to bonded composite repairs applied to metallic aircraft structure. As a part of an Aging Aircraft PA between the USAFRL and DSTO it was agreed to examine three standard treatments applied to aluminium aircraft structure for bonded repairs for the purpose of establishing the long term durability of the treatment in a hot and humid tropical environment. Phosphoric acid anodise (PAA) represents the best standard factory treatment for aluminium, whereas grit-blast and epoxy silane represents a mature surface treatment favoured for in-field repairs. A newer surface treatment using sol-gel chemistry is also being trialled. The sol-gel treatment contains the same epoxy silane, but also takes advantage of unique zirconium chemistry and offers the potential of improving the reliability of the grit-blast and epoxy silane treatment and removing the need for grit-blasting.

More than 100 honeycomb beams have had boron patches bonded to the aluminium skins using FM-300-2K and FM-73 adhesives in two configurations. The two adhesives offer two temperature envelopes for usage and the two patch configurations examine the influence of peel stresses in the critical taper region of the boron reinforcement. Additionally, some beams were patched in which the grit-blast and silane and sol-gel treatments have had some critical steps removed. It is anticipated the effects of removing these steps will enable a more detailed correlation between accelerated durability tests and long term environmental durability to be established.

Initial trials began in December 2003 in which the beams are being loaded to 1800N and patch compliance is being monitored. By early June 2004, more than 180,000 cycles had been completed and only the worst surface treatment samples had provided indications of disbonding, based on strain gauge indications. Tap testing of the strain gauged samples revealed that delaminations at the perimeter of the patch had occurred. The worst surface treatment was an abrade followed by solvent wiping prior to bonding. These samples provided strain gauge indications of disbonding within a few months of the trial beginning and were expected to show poor durability based on accelerated durability trials conducted in the laboratory. Two additional samples have unusual strain gauge readings but do not appear to be linked to sample degradation. NDI measurements of these samples is still required to verify the gauges are no longer functioning.

Loads being applied to the beams have been calculated based on the fatigue life of the core and it is anticipated they should survive for more than 2 million cycles, which will cover the 5 year trial period. At the load being applied the adhesive is conservatively estimated to be loaded at 80% of the elastic limit and should provide a good test for the adhesive bonds. It is expected that over the life of the trial a good indication in relationship between accelerated durability testing and service life performance will be established. The influence of service treatment quality on long term durability should also be provided as a result of the trial.

Further reports are intended over the period of the trial to provide an indication of the surface treatment performance. At the conclusion of the trial it is hoped teardown inspection and residual strength testing of the patched samples will be undertaken to verify the strain gauge results and confirm the relative durability of the surface treatments trialed.

6. December 2004 Update

From the period between 15th of December 2003 and 30th of August 2004, 278,384 cycles were run using a 1800N maximum load. During this period three samples failed in the aluminium skin just outside the patch, as shown in Figure 8, which shows sample 42. Sample 42 (P, BR, NGB, H, 3) failed on the 3/7/04, sample 70 (G, NBR, NGB, L, 3) failed on the 26/7/04 and sample 81 (G, NBR, NGB, H, 7) failed on the 7/9/04,. Initial inspection of the failed samples revealed that fatigue cracking in the skin had initiated from the scratches at the edge of the skin where the beams had been cut to size during manufacture. Cutting had left deep scoring and had clearly led to substantial reduction in the fatigue strength of the aluminium. Approximate calculations suggested that a reduction in skin stress to 30% of yield strength would enable the beams to last the required trial time of 4 years. Additionally, the samples were turned over in order to place the tension skins under compression and try and obviate the reduction in fatigue life that a number of samples would have experienced. As a result of the revised load, strain levels in the adhesive will be around 30% lower than for the original loading used from December 2003 to August 2004. The stress at the end of the patch in the aluminium, σ_{eps} ,will also decrease by 30% and the far field stress in the aluminium, σ_s , should decrease by 40%. Beams will continue to be monitored and should any failures occur during 2005 a more thorough review of the loading conditions in the patches would need to be made. Since the 24th of September 2004 more than 50,000 cycles have been completed without further incident. The average beam compliance monitored with the strain gauges remains around 2.

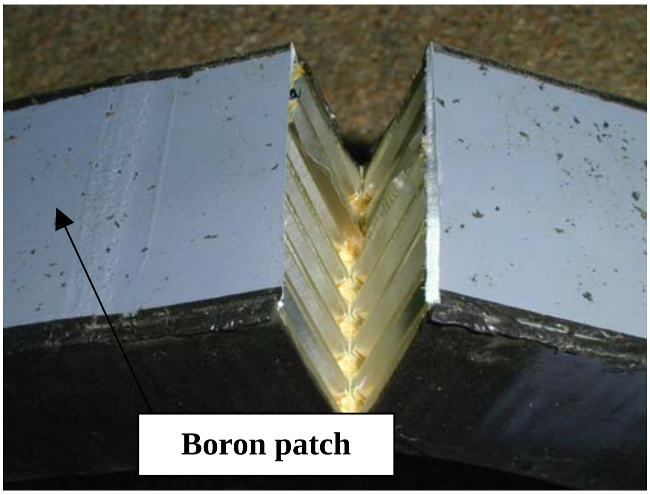

Figure 8 Failed honeycomb beam sample number 42.

Acknowledgments

The support to this program offered by the US Air Force Research Laboratory is acknowledged. Special thanks go to Mr Jim Mazza, Captain Jason Avram, and Lt Heather Crooks of the Materials Directorate for technical input required to get the sandwich beams produced. Support of Mr Dan McCray and colleagues at the University of Dayton Research Institute was also valuable. Captain Mike Myers of Air Vehicles Directorate efforts in providing financial support for specimen manufacture is gratefully acknowledged.

Mr. Bill Schweinberg, Warner Robins Air Logistics Centre, contribution in producing the large aluminium-honeycomb panels at Robins AFB, Georgia and shipment to AFRL at Wright-Patterson AFB, Ohio, for final specimen preparation was crucial in the progress of the project.

Significant DSTO assistance in design and preparation of the beams for testing was provided by Mr Richard Bartholomeusz and Mr Alex Harman. Technical contributions by Mr Peter Haggart in the strain gauging and sealing of the beams cannot be underestimated in the overall importance to the long term success of the project. Initial efforts in planning the project and advice in the latter stages of the project from Dr Richard Chester are also acknowledged. Advice and assistance provided by Mr Noel Goldsmith and Dr Chun Wang in reassessing loads in September 2004 was greatly appreciated.

Appendix A: Test Matrix and Details

A.1. Beam Numbering, Identification and Painting

The beams have been engraved with the number corresponding to the RUN ORDER number in the Beam Test Matrix Table (Table A2), enabling details of each specimen to be traced. After engraving the beams were primed and painted with standard F-111 paint to protect the freshly exposed aluminium.

A.2. Beam Test Matrix

108 beams are used for the trial, all with the honeycomb ribbon oriented at 90 degrees to the length of the beam. 8 beams from the original manufacture remain to be used as dummies which will be required to replace samples in the rigs that fail before the trial ends. Of these 8 samples 6 calibration samples referred to in Appendix B will be used and 2 remaining beams with the PAA treatment will be available.

Table A1 Beams with Silane Surface Treatments missing critical processing steps

Surface treatment Abbreviation	Details of Surface Treatment	Primer	Gritblast	Adhesive
SB	Abrade with scotchbrite and MEK, followed by solvent wipe with tissues and MEK	No	No	FM-73
SBS	Abrade with scotchbrite and MEK, followed by solvent wipe with tissues and MEK, followed by dip in 1% aqueous Silane solution and dry	No	No	FM-73
GB	Abrade with scotchbrite and MEK, followed by solvent wipe with tissues and MEK	No	Yes	FM-73
BS	Perform standard gritblast and silane treatment but use <u>0.5% silane solution instead of 1% silane solution</u>	No	Yes	FM-73

Beam Test Matrix

Table A2 Core running in the width direction of the beam

KEY:

Surface:	P – PAA	SB-scotchbrite abrade	**Grit Blast:**	GB – Grit Blast	NGB – No Grit Blast
	G – Sol-Gel	SBS-scotchbrite abrade+silane	**Patch:**	L – Low Peel Stress	H – High Peel Stress
	S – GBS	GB-gritblast BS-0.5% silane solution	**Adhesive:**	7 – FM-73	3 – FM-300-2
Primer:	BR – Primer	NBR – No Primer			

Run Order	Blocks	Std Order	Surface	Primer	Grit Blast	Patch	Adhesive
83	1	1	P	BR	NGB	L	7
82	1	2	G	NBR	NGB	H	3
78	1	3	S	NBR	GB	H	7
79	1	4	G	BR	GB	L	3
74	1	5	P	BR	NGB	L	7
81	1	6	G	NBR	NGB	H	3
80	1	7	S	NBR	GB	H	7
84	1	8	G	BR	GB	L	3
75	1	9	P	BR	NGB	L	7
76	1	10	G	NBR	NGB	H	3
77	1	11	S	NBR	GB	H	7
73	1	12	G	BR	GB	L	3
7	**2**	**13**	**SB**	**NBR**	**NGB**	**H**	**7**
12	2	14	G	BR	NGB	H	3
3	2	15	S	BR	GB	H	7
9	2	16	G	NBR	GB	L	3
11	**2**	**17**	**SB**	**NBR**	**NGB**	**H**	**7**
2	2	18	G	BR	NGB	H	3
6	2	19	S	BR	GB	H	7
10	2	20	G	NBR	GB	L	3
4	**2**	**21**	**SB**	**NBR**	**NGB**	**H**	**7**
5	2	22	G	BR	NGB	H	3
1	2	23	S	BR	GB	H	7
8	2	24	G	NBR	GB	L	3
58	3	25	P	BR	NGB	L	3
52	3	26	G	NBR	NGB	H	7

Run Order	Blocks	Std Order	Surface	Primer	Grit Blast	Patch	Adhesive
55	3	27	S	NBR	GB	H	3
49	3	28	G	BR	GB	L	7
59	3	29	P	BR	NGB	L	3
51	3	30	G	NBR	NGB	H	7
53	3	31	S	NBR	GB	H	3
57	3	32	G	BR	GB	L	7
56	3	33	P	BR	NGB	L	3
54	3	34	G	NBR	NGB	H	7
50	3	35	S	NBR	GB	H	3
60	3	36	G	BR	GB	L	7
95	**4**	**37**	**SBS**	**NBR**	**NGB**	**H**	**7**
89	4	38	G	BR	NGB	H	7
87	4	39	S	BR	GB	H	3
85	4	40	G	NBR	GB	L	7
92	**4**	**41**	**SBS**	**NBR**	**NGB**	**H**	**7**
94	4	42	G	BR	NGB	H	7
93	4	43	S	BR	GB	H	3
86	4	44	G	NBR	GB	L	7
88	**4**	**45**	**SBS**	**NBR**	**NGB**	**H**	**7**
96	4	46	G	BR	NGB	H	7
90	4	47	S	BR	GB	H	3
91	4	48	G	NBR	GB	L	7
20	**5**	**49**	**GB**	**NBR**	**GB**	**H**	**7**
22	5	50	G	BR	NGB	L	3
17	5	51	S	BR	GB	L	7
18	5	52	G	NBR	GB	H	3
15	**5**	**53**	**GB**	**NBR**	**GB**	**H**	**7**
21	5	54	G	BR	NGB	L	3
16	5	55	S	BR	GB	L	7
23	5	56	G	NBR	GB	H	3
14	**5**	**57**	**GB**	**NBR**	**GB**	**H**	**7**
13	5	58	G	BR	NGB	L	3
24	5	59	S	BR	GB	L	7
19	5	60	G	NBR	GB	H	3
61	6	61	P	BR	NGB	H	7
63	6	62	G	NBR	NGB	L	3
62	6	63	S	NBR	GB	L	7
69	6	64	G	BR	GB	H	3
72	6	65	P	BR	NGB	H	7
67	6	66	G	NBR	NGB	L	3
64	6	67	S	NBR	GB	L	7
65	6	68	G	BR	GB	H	3
66	6	69	P	BR	NGB	H	7
70	6	70	G	NBR	NGB	L	3
68	6	71	S	NBR	GB	L	7
71	6	72	G	BR	GB	H	3
26	**7**	**73**	**BS**	**NBR**	**GB**	**H**	**7**
30	7	74	G	BR	NGB	L	7

Run Order	Blocks	Std Order	Surface	Primer	Grit Blast	Patch	Adhesive
35	7	75	S	BR	GB	L	3
29	7	76	G	NBR	GB	H	7
32	**7**	**77**	**BS**	**NBR**	**GB**	**H**	**7**
27	7	78	G	BR	NGB	L	7
34	7	79	S	BR	GB	L	3
31	7	80	G	NBR	GB	H	7
25	**7**	**81**	**BS**	**NBR**	**GB**	**H**	**7**
33	7	82	G	BR	NGB	L	7
36	7	83	S	BR	GB	L	3
28	7	84	G	NBR	GB	H	7
37	8	85	P	BR	NGB	H	3
39	8	86	G	NBR	NGB	L	7
45	8	87	S	NBR	GB	L	3
40	8	88	G	BR	GB	H	7
38	8	89	P	BR	NGB	H	3
46	8	90	G	NBR	NGB	L	7
43	8	91	S	NBR	GB	L	3
47	8	92	G	BR	GB	H	7
42	8	93	P	BR	NGB	H	3
48	8	94	G	NBR	NGB	L	7
41	8	95	S	NBR	GB	L	3
44	8	96	G	BR	GB	H	7
97	**9**	**97**	**SB**	**NBR**	**NGB**	**L**	**7**
98	**9**	**98**	**SB**	**NBR**	**NGB**	**L**	**7**
99	**9**	**99**	**SB**	**NBR**	**NGB**	**L**	**7**
100	**9**	**100**	**SBS**	**NBR**	**NGB**	**L**	**7**
101	**9**	**101**	**SBS**	**NBR**	**NGB**	**L**	**7**
102	**9**	**102**	**SBS**	**NBR**	**NGB**	**L**	**7**
103	**9**	**103**	**GB**	**NBR**	**GB**	**L**	**7**
104	**9**	**104**	**GB**	**NBR**	**GB**	**L**	**7**
105	**9**	**105**	**GB**	**NBR**	**GB**	**L**	**7**
106	**9**	**106**	**BS**	**NBR**	**GB**	**L**	**7**
107	**9**	**107**	**BS**	**NBR**	**GB**	**L**	**7**
108	**9**	**108**	**BS**	**NBR**	**GB**	**L**	**7**

Table A3 Core running in the width direction of the beam

Run Order	Treatment	Primer	Gritblast	Patch	Adhesive
117	P	BR	NGB	H	7
118	P	BR	NGB	H	7
119	S	BR	GB	H	7
120	S	NBR	GB	H	7
121	G	BR	GB	H	7
122	G	BR	NGB	H	7
123	G	NBR	GB	H	7

Run Order	Treatment	Primer	Gritblast	Patch	Adhesive
124	G	NBR	NGB	H	7
125	SB	NBR	NGB	H	7
126	SBS	NBR	NGB	H	7
127	BS	NBR	GB	H	7
128	GB	NBR	GB	H	7
129	P	BR	NGB	H	3
130	P	BR	NGB	H	3
131	S	BR	GB	H	3
132	S	NBR	GB	H	3
133	G	BR	GB	H	3
134	G	BR	NGB	H	3
135	G	NBR	GB	H	3
136	G	NBR	NGB	H	3
137	SB	NBR	NGB	H	3
138	SBS	NBR	NGB	H	3
139	BS	NBR	GB	H	3
140	GB	NBR	GB	H	3

Appendix B: Beam Positions in Loading Rigs

Table B1

(T-T tension side of beam is top surface, T-B tension side of beam is bottom surface)

Rig Number 1				
Rig Position	**Run Order No. (Gages)**	**Description**		
		Treatment	**Adhesive**	**Patch**
1 (T-T)	75	PAA	FM-73	low
2 (T-B)	49 (3)	Sol-gel, prime, grit-blast	FM-73	low
3 (T-T)	86	Sol-gel, no prime, grit-blast	FM-73	low
4 (T-B)	27	Sol-gel, prime, no grit-blast	FM-73	low
5 (T-T)	46	Sol-gel, no prime, no grit-blast	FM-73	low
6 (T-B)	16	Silane, prime, grit-blast	FM-73	low
7 (T-T)	62 (2)	Silane, no prime, grit-blast	FM-73	low
8 (T-B)	106 (2)	0.5% Silane, no prime, grit-blast	FM-73	low
9 (T-T)	101	SB silane, no prime, no grit-blast	FM-73	low
10 (T-B)	105	Grit-blast	FM-73	low
11 (T-T)	99	Scotchbrite	FM-73	low
12 (T-B)	18 (3)	Sol-gel, no prime, grit-blast	FM-300-2	high

Rig Number 2				
Rig Position	**Run Order No. (Gages)**	**Description**		
		Treatment	**Adhesive**	**Patch**
7 (T-T)	74 (2)	PAA	FM-73	low
8 (T-B)	57	Sol-gel, prime, grit-blast	FM-73	low
9 (T-T)	85 (2)	Sol-gel, no prime, grit-blast	FM-73	low
10 (T-B)	30 (2)	Sol-gel, prime, no grit-blast	FM-73	low
11 (T-T)	39 (2)	Sol-gel, no prime, no grit-blast	FM-73	low
12 (T-B)	17	Silane, prime, grit-blast	FM-73	low
1 (T-T)	64	Silane, no prime, grit-blast	FM-73	low
2 (T-B)	107	0.5% Silane, no prime, grit-blast	FM-73	low
3 (T-T)	102	SB silane, no prime, no grit-blast	FM-73	low
4 (T-B)	104	Grit-blast	FM-73	low
5 (T-T)	98	Scotchbrite	FM-73	low
6 (T-B)	8 (2)	Sol-gel, no prime, grit-blast	FM-300-2	low

(T-T tension side of beam is top surface, T-B tension side of beam is bottom surface)

Rig Number 3				
Rig Position	**Run Order No. (Gages)**	**Description**		
		Treatment	**Adhesive**	**Patch**
12 (T-B)	83	PAA	FM-73	low
11 (T-T)	60	Sol-gel, prime, grit-blast	FM-73	low
10 (T-B)	91	Sol-gel, no prime, grit-blast	FM-73	low
9 (T-T)	33	Sol-gel, prime, no grit-blast	FM-73	low
8 (T-B)	48	Sol-gel, no prime, no grit-blast	FM-73	low
7 (T-T)	24 (2)	Silane, prime, grit-blast	FM-73	low
6 (T-B)	68	Silane, no prime, grit-blast	FM-73	low
5 (T-T)	108	0.5% Silane, no prime, grit-blast	FM-73	low
4 (T-B)	100 (2)	SB silane, no prime, no grit-blast	FM-73	low
3 (T-T)	103 (2)	Grit-blast	FM-73	low
2 (T-B)	97 (2)	Scotchbrite	FM-73	low
1 (T-T)	73 (2)	Sol-gel, prime, grit-blast	FM-300-2	low

Rig Number 4				
Rig Position	**Run Order No. (Gages)**	**Description**		
		Treatment	**Adhesive**	**Patch**
1 (T-T)	61 (2)	PAA	FM-73	high
2 (T-B)	40 (2)	Sol-gel, prime, grit-blast	FM-73	high
3 (T-T)	29	Sol-gel, no prime, grit-blast	FM-73	high
4 (T-B)	94	Sol-gel, prime, no grit-blast	FM-73	high
5 (T-T)	52	Sol-gel, no prime, no grit-blast	FM-73	high
6 (T-B)	1 (2)	Silane, prime, grit-blast	FM-73	high
7 (T-T)	77 (2)	Silane, no prime, grit-blast	FM-73	high
8 (T-B)	32	0.5% Silane, no prime, grit-blast	FM-73	high
9 (T-T)	95	SB silane, no prime, no grit-blast	FM-73	high
10 (T-B)	20	Grit-blast	FM-73	high
11 (T-T)	7	Scotchbrite	FM-73	high
12 (T-B)	65 (2)	Sol-gel, prime, grit-blast	FM-300-2	high

(T-T tension side of beam is top surface, T-B tension side of beam is bottom surface)

Rig Number 5				
Rig Position	Run Order No. (Gages)	Description		
		Treatment	Adhesive	Patch
7 (T-T)	66	PAA	FM-73	high
8 (T-B)	44	Sol-gel, prime, grit-blast	FM-73	high
9 (T-T)	31	Sol-gel, no prime, grit-blast	FM-73	high
10 (T-B)	96	Sol-gel, prime, no grit-blast	FM-73	high
11 (T-T)	51 (2)	Sol-gel, no prime, no grit-blast	FM-73	high
12 (T-B)	3	Silane, prime, grit-blast	FM-73	high
1 (T-T)	78	Silane, no prime, grit-blast	FM-73	high
2 (T-B)	25 (3)	0.5% Silane, no prime, grit-blast	FM-73	high
3 (T-T)	92	SB silane, no prime, no grit-blast	FM-73	high
4 (T-B)	15	Grit-blast	FM-73	high
5 (T-T)	4 (3)	Scotchbrite	FM-73	high
6 (T-B)	50 (2)	Silane, no prime, grit-blast	FM-300-2	high

Rig Number 6				
Rig Position	Run Order No. (Gages)	Description		
		Treatment	Adhesive	Patch
12 (T-B)	72	PAA	FM-73	high
11 (T-T)	47	Sol-gel, prime, grit-blast	FM-73	high
10 (T-B)	28 (2)	Sol-gel, no prime, grit-blast	FM-73	high
9 (T-T)	89 (2)	Sol-gel, prime, no grit-blast	FM-73	high
8 (T-B)	54	Sol-gel, no prime, no grit-blast	FM-73	high
7 (T-T)	6	Silane, prime, grit-blast	FM-73	high
6 (T-B)	80	Silane, no prime, grit-blast	FM-73	high
5 (T-T)	26	0.5% Silane, no prime, grit-blast	FM-73	high
4 (T-B)	88 (3)	SB silane, no prime, no grit-blast	FM-73	high
3 (T-T)	14 (3)	Grit-blast	FM-73	high
2 (T-B)	11	Scotchbrite	FM-73	high
1 (T-T)	71	Sol-gel, prime, grit-blast	FM-300-2	high

(T-T tension side of beam is top surface, T-B tension side of beam is bottom surface)

Rig Number 7				
Rig Position	Run Order No (Gages)	Description		
		Treatment	Adhesive	Patch
1 (T-T)	58	PAA	FM-300-2	low
2 (T-B)	79	Sol-gel, prime, grit-blast	FM-300-2	low
3 (T-T)	5(1)	Sol-gel, prime, no grit-blast	FM-300-2	high
4 (T-B)	67	Sol-gel, no prime, no grit-blast	FM-300-2	low
5 (T-T)	35	Silane, prime, grit-blast	FM-300-2	low
6 (T-B)	43	Silane, no prime, grit-blast	FM-300-2	low
7 (T-T)	37	PAA	FM-300-2	high
8 (T-B)	13 (2)	Sol-gel, prime, no grit-blast	FM-300-2	low
9 (T-T)	2 (3)	Sol-gel, prime, no grit-blast	FM-300-2	high
10 (T-B)	76 (3)	Sol-gel, no prime, no grit-blast	FM-300-2	high
11 (T-T)	87 (2)	Silane, prime, grit-blast	FM-300-2	high
12 (T-B)	69	Sol-gel, prime, grit-blast	FM-300-2	high

Rig Number 8				
Rig Position	Run Order No	Description		
		Treatment	Adhesive	Patch
7 (T-T)	56 (2)	PAA	FM-300-2	low
8 (T-B)	9	Sol-gel, no prime, grit-blast	FM-300-2	low
9 (T-T)	21	Sol-gel, prime, no grit-blast	FM-300-2	low
10 (T-B)	63 (2)	Sol-gel, no prime, no grit-blast	FM-300-2	low
11 (T-T)	34 (2)	Silane, prime, grit-blast	FM-300-2	low
12 (T-B)	41 (2)	Silane, no prime, grit-blast	FM-300-2	low
1 (T-T)	38 (2)	PAA	FM-300-2	high
2 (T-B)	19	Sol-gel, no prime, grit-blast	FM-300-2	high
3 (T-T)	84	Sol-gel, prime, grit-blast	FM-300-2	low
4 (T-B)	81	Sol-gel, no prime, no grit-blast	FM-300-2	high
5 (T-T)	90	Silane, prime, grit-blast	FM-300-2	high
6 (T-B)	53	Silane, no prime, grit-blast	FM-300-2	high

(T-T tension side of beam is top surface, T-B tension side of beam is bottom surface)

Rig Number 9				
Rig Position	**Run Order No.**	**Description**		
		Treatment	**Adhesive**	**Patch**
12 (T-B)	59	PAA	FM-300-2	low
11 (T-T)	10	Sol-gel, no prime, grit-blast	FM-300-2	low
10 (T-B)	22	Sol-gel, prime, no grit-blast	FM-300-2	low
9 (T-T)	70	Sol-gel, no prime, no grit-blast	FM-300-2	low
8 (T-B)	36	Silane, prime, grit-blast	FM-300-2	low
7 (T-T)	45	Silane, no prime, grit-blast	FM-300-2	low
6 (T-B)	42	PAA	FM-300-2	high
5 (T-T)	23	Sol-gel, no prime, grit-blast	FM-300-2	high
4 (T-B)	12	Sol-gel, prime, no grit-blast	FM-300-2	high
3 (T-T)	82	Sol-gel, no prime, no grit-blast	FM-300-2	high
2 (T-B)	93	Silane, prime, grit-blast	FM-300-2	high
1 (T-T)	55	Silane, no prime, grit-blast	FM-300-2	high

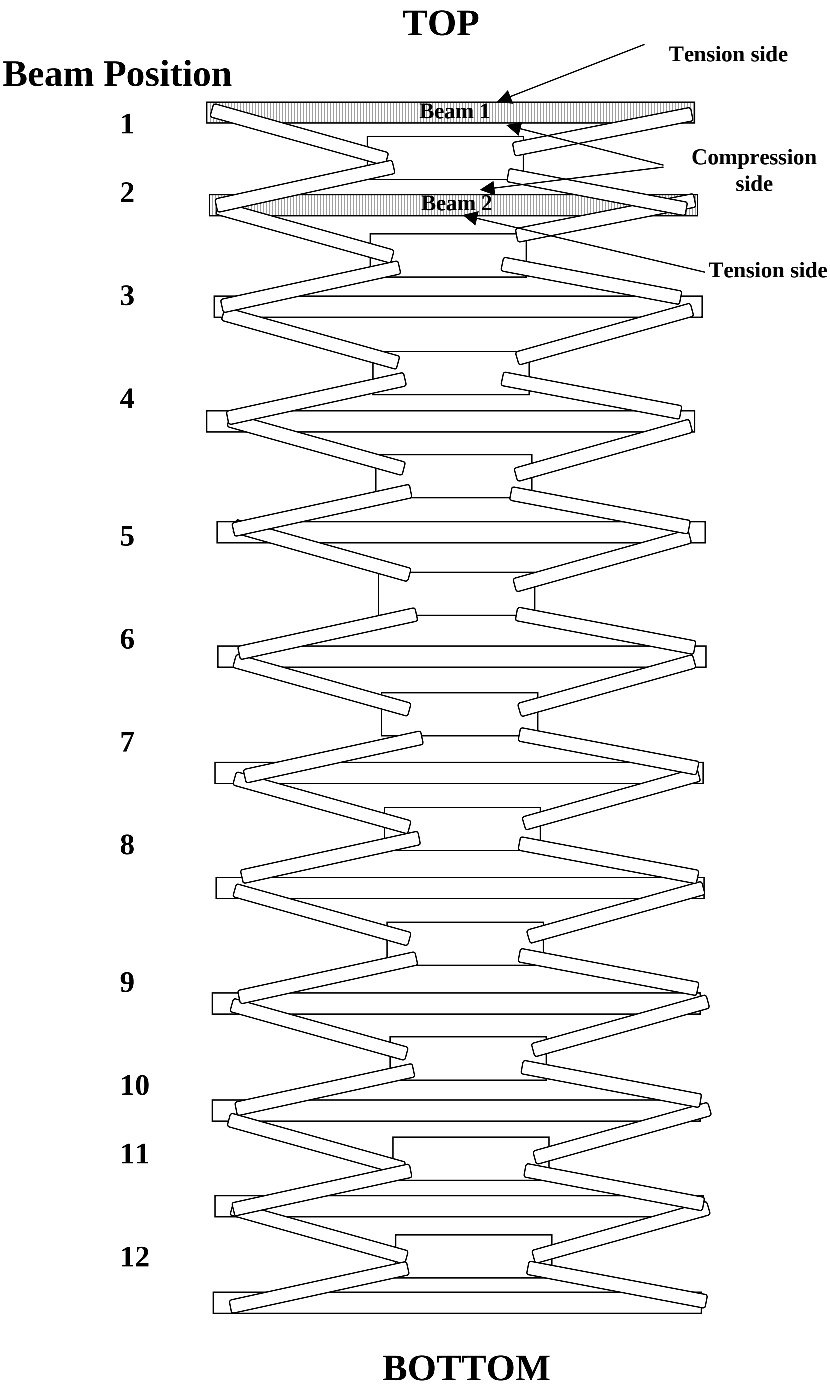

Figure B1 Beam position identification in loading rig (Side view)

Appendix C: Gauge positions on Beams

Table C1 Gauge positions on beams

Run Order No.	Treatment	Number of Gauges	Gauge Location
1	S,BR,GB,H,7	2	C, T
2	G,BR,NGB,H,3	3	C, T1, T2
4	SB, NBR, NGB, H, 7	3	C, T1, T2
8	G, NBR, GB, L, 3	2	C, T
13	G, BR, NGB, L, 3	2	C, T
14	GB,NBR,GB,H,7	3	C, T1, T2
18	G, NBR, GB, H, 3	3	C, T1, T2
24	S, BR, GB, L, 7	2	C, T
25	BS,NBR,GB,H,7	3	C, T1, T2
28	G, NBR, GB, H, 7	2	C, T
30	G, BR, NGB, L, 7	2	C, T
34	S, BR, GB, L, 3	2	C, T
38	P, BR, NGB, H, 3	2	C, T
39	G, NBR, NGB, L, 7	2	C, T
40	G,BR,GB,H,7	2	C, T
41	S, NBR, GB, L, 3	2	C, T
49	G, BR, GB, L, 7	3	C, T1, T2
50	S, NBR, GB, H, 3	2	C, T
51	G, NBR, NGB, H, 7	2	C, T
56	P, BR, NGB, L, 3	2	C, T
61	P, BR, NGB, H, 7	2	C, T
62	S,NBR,GB,L,7	2	C, T
63	G, NBR, NGB, L, 3	2	C, T
65	G, BR, GB, H, 3	2	C, T
73	G, BR, GB, L, 3	2	C, T
74	P, BR, NGB, L, 7	2	C, T
76	G,NBR,NGB,H,3	3	C, T1, T2
77	S, NBR, GB, H, 7	2	C, T
85	G, NBR, GB, L, 7	2	C, T
87	S, BR, GB, H, 3	2	C, T
88	SBS, NBR, NGB, H, 7	3	C, T1, T2
89	G, BR, NGB, H, 7	2	C, T
97	SB, NBR, NGB, L, 7	2	C, T
100	SBS, NBR, NGB, L, 7	2	C, T
103	GB, NBR, GB, L, 7	2	C, T
106	BS, NBR, GB, L, 7	2	C, T

C-compression side, T-tension side (close to patch termination), T1-tension side (close to patch termination-position 1), T2-tension side (close to patch termination-position 2). Refer to Figure C1 for details.

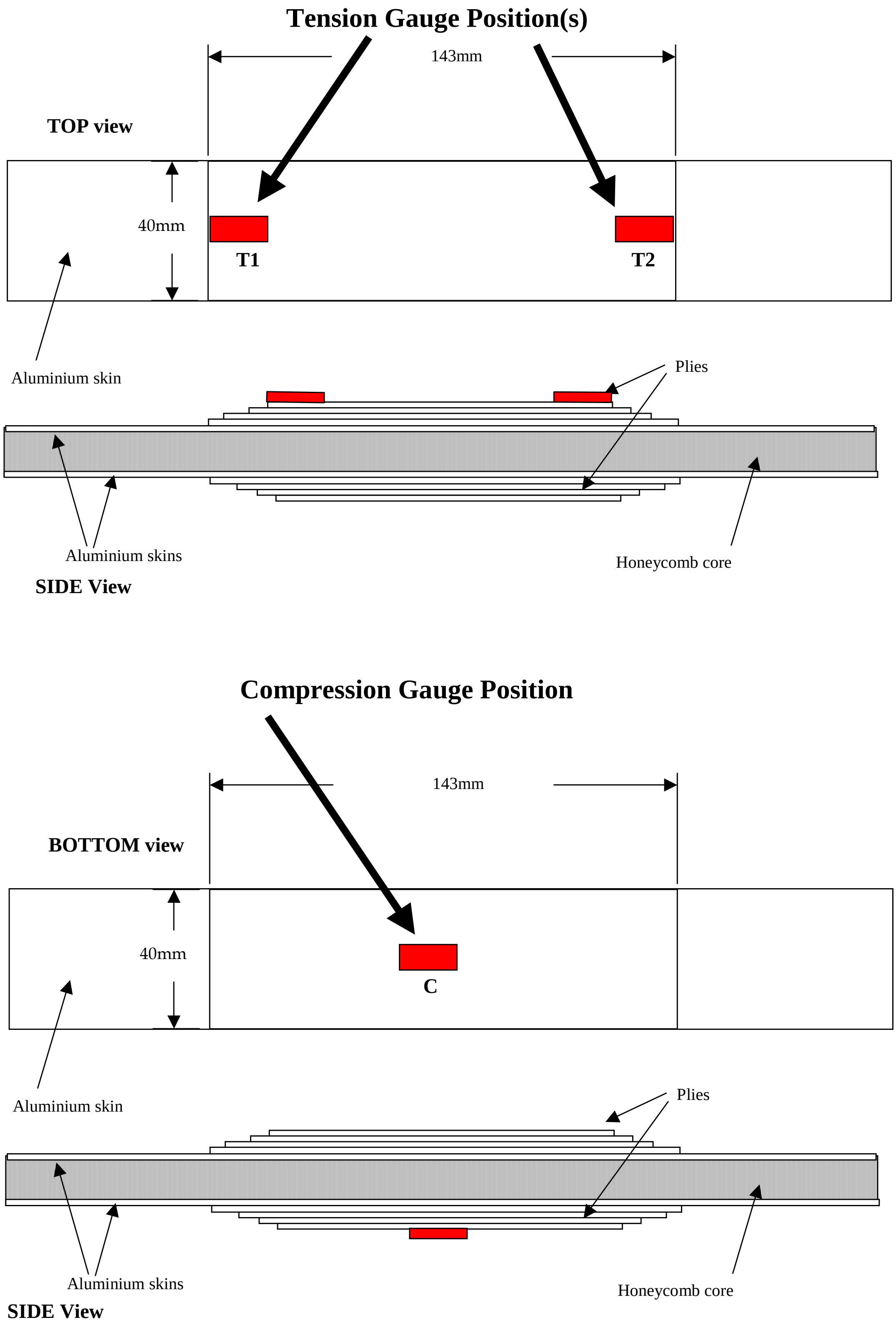

Figure C1 Tension and compression side gauge positions.

Appendix D: Calibration Beams and Measured Strains

Table D1 Surface treatments used for calibration beams

Description	Number
Adhesive: FM-73 Surface Prep: PAA (P) primer (BR) Patch: High Peel Stress (H) Honeycomb Direction: Ribbon Perpendicular to Length	3
Adhesive: FM-73 Surface Prep: PAA (P) primer (BR) Patch: Low Peel Stress (L) Honeycomb Direction: Ribbon Perpendicular to Length	3

Table D2 Strain Gauge readings and equivalent stress for high and low peel stress patches on honeycomb beams bonded with FM73 adhesive.

Patch	Temp (°C)	Strain Gauge Position	Slope (N/ε)	Error	Strain at 1800N (με)	Error	Equivalent Stress (ksi)	Stress from 7021. 016-1 (ksi)[3]
Low Peel, FM73	25	Tension, Boron, Patch run-off	4.7	0.9	383	60	11.5	30
		Compression, Boron, patch centre	4.3	0.1	419	10	12.6	14
		Tension, Aluminium, patch perimeter	1.8	0.1	1000	40	10.5	30
Low Peel, FM73	80	Tension, Boron, patch run-off	11	2	164	36	4.9	20
		Compression, Boron, patch centre	5.2	0.3	346	20	10.4	9.4
		Tension, Aluminium, patch perimeter	1.7	0.1	1059	70	11.1	20
High Peel, FM73	25	Tension, Boron, patch run-off	5.6	0.4	321	25	9.6	30
		Compression, Boron, patch centre	4.3	0.1	419	10	12.6	14
		Tension, Aluminium, patch perimeter	1.9	0.1	947	50	9.9	30
High Peel, FM73	80	Tension, Boron, patch run-off	16	2	113	20	3.4	20
		Compression, Boron, patch centre	4.9	1	367	60	11.0	9.4
		Tension, Aluminium, patch perimeter	1.8	0.2	1000	100	10.5	20

[3] Australian Air Publication 7021.016-1, "Composite and Adhesive Bonded Repairs, Engineering and Design Procedures", Royal Australian Air Force, 2003, refer Appendix E and F.

Appendix E: Static Stresses Calculated for the FM300-2K Bonded Boron-Epoxy Patches[17]

$\eta := 0.006$ **inch**

$G := 70000$ **psi**

$\tau_p := 6700$ **psi**

ElasticModulus

$E_c := G \cdot 2 \cdot (1 + 0.33)$ $E_c = 1.862 \times 10^5$ **psi**

Cure Temperature

$T_{cure} := 250$ **F for 2 hr**

AdhesiveStrain Limit

Elastic $\gamma_e := 0.0957$ **Plastic** $\gamma_{fail} := 0.190$

Operating Temperature

$T_{oper} := 77$ **F**

$\gamma_p := \gamma_{fail} - \gamma_e$

$\gamma_p = 0.094$

Input Structure Material

2024-T3 Aluminium Alloy

$t_i := 0.05$ **in**

Yield Stress

Thermal Expansion Coefficient

Ultimate Stress

$\sigma_{yi} := 44000$ **psi**

$\alpha_i := 12.7 \cdot 10^{-6}$ **in/in/F**

$\sigma_{ui} := 64000$ **psi**

Poisson's Ratio

Applied Local Strain

Elastic Modulus

$\nu_i := 0.33$

$\varepsilon_a := 1000 \cdot 10^{-6}$

$E_i := 10.5 \cdot 10^6$ **psi**

Fracture toughness

$K_c := 83500$

$\sigma_a := \varepsilon_a \cdot E_i$ $\sigma_a = 1.05 \times 10^4$

$$\alpha_{ieff} := \frac{\alpha_i \cdot (1 + \nu_i)}{2}$$

Patch Material Properties:

Boron Epoxy 5521 Composite

Elastic Modulus

Thermal Expansion Coefficient

Shear Modulus

$E_o := 30.0 \cdot 10^6$ **psi**

$\alpha_o := 2.3 \cdot 10^{-6}$ **in/in/F**

$G_o := .7 \cdot 10^6$ **psi**

Ply Thickness

Longitudinal Strength

Ultimate Longitudinal Strain

$t_{ply} := 0.0052$

$\sigma_L := 192 \cdot 10^3$ **psi**

$$\varepsilon_o := \frac{\sigma_L}{E_o}$$

$\varepsilon_o = 6.4 \times 10^{-3}$

t_0=0.0208 (4 plies)

Maximum Shear Strain In Adhesive Assuming All Load Transferred into the Patch

$$\gamma_{\mathbf{adh}} := 0.064$$

$$\mathbf{G} := 70000\ \mathbf{psi} \qquad \tau_{\mathbf{a}} := \mathbf{G}\cdot\gamma_{\mathbf{adh}}$$

$$\tau_{\mathbf{a}} = 4.48\times 10^{3}\ \ \mathbf{psi} \qquad \tau_{\mathbf{a}}\cdot 0.00689 = 30.867\ \ \mathbf{MPa}$$

$$\lambda := \sqrt{\frac{\mathbf{G}}{\eta}\cdot\left(\frac{1}{\mathbf{E_i}\cdot\mathbf{t_i}} + \frac{1}{\mathbf{E_o}\cdot\mathbf{t_o}}\right)} \qquad \lambda = 6.397$$

Stress under the patch (middle) in the Structure (aluminium)

$$\sigma_{\mathbf{ups}} := \frac{\gamma_{\mathbf{adh}}\cdot\mathbf{G}}{\left(\mathbf{t_i}\cdot\lambda\right)} \qquad \sigma_{\mathbf{ups}} = 1.401\times 10^{4}\ \ \mathbf{psi}$$

Stress at the end of the patch in the Structure (aluminium)

$$\sigma_{\mathbf{eps}} := \frac{\sigma_{\mathbf{ups}}\cdot\left(\mathbf{E_o}\cdot\mathbf{t_o} + \mathbf{E_i}\cdot\mathbf{t_i}\right)}{\left(\mathbf{E_i}\cdot\mathbf{t_i}\right)} \qquad \sigma_{\mathbf{eps}} = 3.066\times 10^{4}\ \ \mathbf{psi}$$

Load Attraction Factor

$$\Omega_{\mathbf{L}} := 1.26$$

From AAP 7021.016-1 Table 6.C.1-1 assuming L/w=3.6 and Eoto/Eiti=1.2

Residual Stresses Due to Thermal Expansion Mismatch

$$\sigma_{\mathbf{tem}} := \mathbf{E_i}\cdot\left[\left(\alpha_{\mathbf{o}} - \alpha_{\mathbf{i}}\right)\cdot\left(75 - \mathbf{T_{cure}}\right) + \left(\alpha_{\mathbf{o}} - \alpha_{\mathbf{i}}\right)\cdot\left(\mathbf{T_{oper}} - 75\right)\right]$$

$$\sigma_{\mathbf{tem}} = 1.889\times 10^{4}\ \ \mathbf{psi}$$

Far field stress in the aluminium skin

$$\sigma_{\mathbf{s}} := \frac{\sigma_{\mathbf{eps}} - \left[\mathbf{E_i}\cdot\left[\left(\alpha_{\mathbf{o}} - \alpha_{\mathbf{ieff}}\right)\cdot\left(75 - \mathbf{T_{cure}}\right) + \left(\alpha_{\mathbf{o}} - \alpha_{\mathbf{i}}\right)\cdot\left(\mathbf{T_{oper}} - 75\right)\right]\right]}{\Omega_{\mathbf{L}}}$$

$$\sigma_{\mathbf{s}} = 1.554\times 10^{4}\ \ \mathbf{psi}$$

==

STEP (ALEX): CALCULATE THE LOAD TO ACHIEVE σ_f

Beam Properties

Core thickness $\mathbf{c} := 1$ in

Sandwich Thickness $\mathbf{d} := \mathbf{c} + 2\cdot\mathbf{t_i}$ in

Sandwich Width $\mathbf{b} := 1.575$ in

Beam Length $\mathbf{length} := 25$ in

Loads

Internal Moment

$$\mathbf{M} := \sigma_{\mathbf{s}}\cdot\left[\mathbf{t_i}\cdot\mathbf{b}\cdot\frac{(\mathbf{d}+\mathbf{c})}{2}\right]$$

Refer to ASTM C393

$\mathbf{M} = 1.285\times 10^3$ lb.in

Applied Load (1/4 point bend test - M=PL/8)

Note: Far field stress taken between the load applicators

$$\mathbf{P} := 8\cdot\frac{\mathbf{M}}{\mathbf{length}} \qquad \mathbf{P} = 411.211 \quad \text{lb}$$

$\mathbf{lb2N} := 4.448$

$\mathbf{P_{newtons}} := \mathbf{P}\cdot\mathbf{lb2N}$

$\mathbf{P_{newtons}} = 1.829\times 10^3$ N

Appendix F: Static Stresses Calculated for the FM73 Bonded Boron-Epoxy Patches [17]

FM73 Wet (250 F Autoclave Cure) Using 75 operating temperature data max loa
MDC 91B0330 dated 30 Jun 91

Adhesive Thickness

$\eta := 0.0045$ **inch** $\quad G := 47380$ **psi**

Adhesive Shear Stress

$\tau_p := 4845$ **psi**

ElasticModulus

$E_c := G\cdot 2\cdot(1 + 0.33)$ $\quad E_c = 1.26\times 10^5$ **psi** $\quad T_{cure} := 250$

Operating Temperature

$T_{oper} := 90$ **F**

AdhesiveStrain Limit

Elastic $\quad \gamma_e := 0.102 \quad \gamma_{fail} := 0.756$

Plastic $\quad \gamma_p := \gamma_{fail} - \gamma_e \quad \gamma_p = 0.654$

Input Structure Material

2024-T3 Aluminium Alloy

$t_i := 0.05$ **in**

Ultimate Stress

$\sigma_{ui} := 64000$ **psi**

Elastic Modulus

$E_i := 10.5\cdot 10^6$ **psi**

Yield Stress

$\sigma_{yi} := 44000$ **psi**

Poisson's Ratio

$\nu_i := 0.33$

Fracture toughness

$K_c := 83500$

Thermal Expansion Coefficient

$\alpha_i := 12.7\cdot 10^{-6}$ **in/in/F**

Applied Local Strain

$\varepsilon_a := 1000\cdot 10^{-6}$

$\sigma_a := \varepsilon_a\cdot E_i \quad \sigma_a = 1.05\times 10^4$

$$\alpha_{ieff} := \frac{\alpha_i\cdot(1 + \nu_i)}{2}$$

Patch Material Properties:

Boron Epoxy 5521 Composite

Elastic Modulus

$E_o := 30.0\cdot 10^6$ **psi**

Thermal Expansion Coefficient

$\alpha_o := 2.3\cdot 10^{-6}$ **in/in/F**

Shear Modulus

$G_o := .7\cdot 10^6$ **psi**

Ply Thickness

$t_{ply} := 0.0052$

Longitudinal Strength

$\sigma_L := 192\cdot 10^3$ **psi**

Ultimate Longitudinal Strain

$$\varepsilon_o := \frac{\sigma_L}{E_o}$$

t_0=0.0208 (4 plies)

$\varepsilon_o = 6.4\times 10^{-3}$

Maximum Shear Strain In Adhesive Assuming All Load Transferred into the Patch

$$\gamma_{adh} := 0.085$$

$$G := 47380 \text{ psi} \qquad \tau_a := G \cdot \gamma_{adh}$$

$$\tau_a = 4.027 \times 10^3 \text{ psi} \qquad \tau_a \cdot 0.00689 = 27.748 \text{ MPa}$$

$$\lambda := \sqrt{\frac{G}{\eta} \cdot \left(\frac{1}{E_i \cdot t_i} + \frac{1}{E_o \cdot t_o} \right)} \qquad \lambda = 6.077$$

Stress under the patch (middle) in the Structure (aluminium)

$$\sigma_{ups} := \frac{\gamma_{adh} \cdot G}{(t_i \cdot \lambda)} \qquad \sigma_{ups} = 1.325 \times 10^4 \text{ psi}$$

Stress at the end of the patch in the Structure (aluminium)

$$\sigma_{eps} := \frac{\sigma_{ups} \cdot (E_o \cdot t_o + E_i \cdot t_i)}{(E_i \cdot t_i)} \qquad \sigma_{eps} = 2.901 \times 10^4 \text{ psi}$$

Load Attraction Factor

$\Omega_L := 1.26$ From AAP 7021.016-1 Table 6.C.1-1 assuming L/w=3.6 and Eoto/Eiti=1.2

Residual Stresses Due to Thermal Expansion Mismatch

$$\sigma_{tem} := E_i \cdot \left[(\alpha_o - \alpha_i) \cdot (75 - T_{cure}) + (\alpha_o - \alpha_i) \cdot (T_{oper} - 75) \right]$$

$$\sigma_{tem} = 1.747 \times 10^4 \text{ psi}$$

Far field stress in the aluminium skin

$$\sigma_s := \frac{\sigma_{eps} - \left[E_i \cdot \left[(\alpha_o - \alpha_{ieff}) \cdot (75 - T_{cure}) + (\alpha_o - \alpha_i) \cdot (T_{oper} - 75) \right] \right]}{\Omega_L}$$

$$\sigma_s = 1.536 \times 10^4 \text{ psi}$$

==

STEP (ALEX): CALCULATE THE LOAD TO ACHIEVE σ_f

Beam Properties

Core thickness $\mathbf{c} := 1$ in

Sandwich Thickness $\mathbf{d} := \mathbf{c} + 2 \cdot \mathbf{t_i}$ in

Sandwich Width $\mathbf{b} := 1.575$ in

Beam Length $\mathbf{length} := 25$ in

Loads

Internal Moment $\mathbf{M} := \sigma_{\mathbf{s}} \cdot \left[\mathbf{t_i} \cdot \mathbf{b} \cdot \frac{(\mathbf{d} + \mathbf{c})}{2} \right]$

Refer to ASTM C393 $\mathbf{M} = 1.27 \times 10^3$ lb.in

Applied Load (1/4 point bend test - M=PL/8)

Note: Far field stress taken between the load applicators

$\mathbf{P} := 8 \cdot \frac{\mathbf{M}}{\mathbf{length}}$ $\mathbf{P} = 406.437$ lb

$\mathbf{lb2N} := 4.448$

$\mathbf{P_{newtons}} := \mathbf{P} \cdot \mathbf{lb2N}$

$\mathbf{P_{newtons}} = 1.808 \times 10^3$ N

References

[1] "Advances in Bonded Composite Repair of Metallic Aircraft Structure", Ed. Baker, A.A., Rose, L.R.F., Jones, R., Vol 1-2, Elsevier, United Kingdom, 2002.

[2] Baker, A. A., "Repair of Cracked or Defective Metallic Aircraft Components with Advanced Fibre Composites-an Overview of Australian Work", Composite Structures, 2, 153-181, 1984.

[3] Walker, K.F. and Rose, L.R. F., in "Advances in Bonded Composite Repair of Metallic Aircraft Structure", Ed. Baker, A.A., Rose, L.R.F., Jones, R., Vol 2, Chapter 27, page 797-811, Elsevier, United Kingdom, 2002.

[4] Schweinberg, W. H., and Fiebig, J. W., in "Advances in Bonded Composite Repair of Metallic Aircraft Structure", Ed. Baker, A.A., Rose, L.R.F., Jones, R., Vol 1, Chapter 41, page 1009-1032, Elsevier, United Kingdom, 2002.

[5] Baker, AA, Chester, RJ. Int J Adhesion and Adhesives, 12, 73, 1992.

[6] Kuhbander, RJ, Mazza, JP. In: Proc. 38th Int SAMPE Symp., 38, 1225, 1993.

[7] Venables, JD, J Mater Sci., 19, 2431, 1984.

[8] Pergan, I., Int J. Adhesion and Adhesives, 19 (1999) 199.

[9] Locke, MC and Scardino, WM, Phosphoric Acid Non-Tank Anodise (PANTA) Process for Repair Bonding, Proceedings of , pp218-241.

[10] Davis, M J, Roberts, J D, "Procedure for Application of Boron-Fibre Reinforced Plastic Patch to the Mirage Lower Wing Skin Fuel Decant Region", ARL-MAT-TECH-MEMO-373, August 1981, DSTO, Australia.

[11] Rider, AN, Chalkley, PD. Int J Adhesion and Adhesives, 24, 95-106, 2004.

[12] AC Tech 7341 Anaconda Avenue, CA 92841, USA

[13] Chalkley, PD, Chester, RJ. "Interim Report on Environmental Program-Durability of Graphite/Epoxy Honeycomb Specimens with Representative Damage and Repairs", Aircraft Materials Technical Memorandum 397, DSTO, Melbourne, July 1988.

[14] "F/A-18 Fatigue Evaluation of Phosphoric Anodized (PAA) Aluminum Honeycomb Core", Report Boeing-STL 00A0047, 28 July, 2000.

[15] "Bonded Honeycomb Sandwich Construction", TSB124, Hexcel Corporation.

[16] Rider, AN , Arnott, DR , Surf Interface Anal, 24, 583, 1996.

[17] Australian Air Publication 7021.016-1, "Composite and Adhesive Bonded Repairs, Engineering and Design Procedures", Royal Australian Air Force, 2003

DISTRIBUTION LIST

Environmental Durability Trial of Bonded Composite Repairs to Metallic Aircraft Structure

Andrew Rider, Ian Williams Ed Shum and Leo Mirabella

AUSTRALIA

DEFENCE ORGANISATION	**No. of copies**
Task Sponsor	
ASI-4A Dr Madabhushi Janardhana(Jana)	1 Printed
ASI-4D Mr Max Davis	1 Printed
S&T Program	
Chief Defence Scientist	1
Deputy Chief Defence Scientist Policy	1
AS Science Corporate Management	1
Director General Science Policy Development	1
Counsellor Defence Science, London	Doc Data Sheet
Counsellor Defence Science, Washington	Doc Data Sheet
Scientific Adviser to MRDC, Thailand	Doc Data Sheet
Scientific Adviser Joint	1
Navy Scientific Adviser	Doc Data Sheet
Scientific Adviser – Army	Doc Data Sheet
Air Force Scientific Adviser	1
Scientific Adviser to the DMO	Doc Data Sheet
Platforms Sciences Laboratory	
Deputy Chief Defence Scientist Aerospace	Doc Data Sht & Exec Summ
Chief of Air Vehicles Division	Doc Data Sht & Dist List
Research Leader Aircraft Materials	1 Printed
Chun Wang	1 Printed
Andrew Rider	1 Printed
Ian Williams	1 Printed
DSTO Library and Archives	
Library Fishermans Bend	Doc Data Sheet
Library Edinburgh	1 printed
Defence Archives	1 printed
Capability Development Group	
Director General Maritime Development	Doc Data Sheet
Director General Land Development	1

Director General Capability and Plans	Doc Data Sheet
Assistant Secretary Investment Analysis	Doc Data Sheet
Director Capability Plans and Programming	Doc Data Sheet
Chief Information Officer Group	
Director General Australian Defence Simulation Office	Doc Data Sheet
AS Information Strategy and Futures	Doc Data Sheet
Director General Information Services	Doc Data Sheet
Strategy Group	
Director General Military Strategy	Doc Data Sheet
Assistant Secretary Governance and Counter-Proliferation	Doc Data Sheet
Navy	
Maritime Operational Analysis Centre, Building 89/90 Garden Island Sydney NSW	Doc Data Sht & Dist List
Deputy Director (Operations)	
Deputy Director (Analysis)	
Director General Navy Capability, Performance and Plans, Navy Headquarters	Doc Data Sheet
Director General Navy Strategic Policy and Futures, Navy Headquarters	Doc Data Sheet
Air Force	
SO (Science) - Headquarters Air Combat Group, RAAF Base, Williamtown NSW 2314	Doc Data Sht & Exec Summ
Army	
ABCA National Standardisation Officer	e-mailed Doc Data Sheet
Land Warfare Development Sector, Puckapunyal	
SO (Science) - Land Headquarters (LHQ), Victoria Barracks NSW	Doc Data & Exec Summary
SO (Science), Deployable Joint Force Headquarters (DJFHQ) (L), Enoggera QLD	Doc Data Sheet
Joint Operations Command	
Director General Joint Operations	Doc Data Sheet
Chief of Staff Headquarters Joint Operations Command	Doc Data Sheet
Commandant ADF Warfare Centre	Doc Data Sheet
Director General Strategic Logistics	Doc Data Sheet
COS Australian Defence College	Doc Data Sheet
Intelligence and Security Group	
AS Concepts, Capability and Resources	1
DGSTA , Defence Intelligence Organisation	1 Printed
Manager, Information Centre, Defence Intelligence Organisation	1
Director Advanced Capabilities	Doc Data Sheet
Defence Materiel Organisation	
Deputy CEO	Doc Data Sheet

Head Aerospace Systems Division	Doc Data Sheet
Head Maritime Systems Division	Doc Data Sheet
Program Manager Air Warfare Destroyer	Doc Data Sheet
CDR Joint Logistics Command	Doc Data Sheet
Guided Weapon & Explosive Ordnance Branch (GWEO)	Doc Data Sheet
OTHER ORGANISATIONS	
National Library of Australia	1
NASA (Canberra)	1
UNIVERSITIES AND COLLEGES	
Australian Defence Force Academy	
Library	1
Head of Aerospace and Mechanical Engineering	1
Hargrave Library, Monash University	Doc Data Sheet
OUTSIDE AUSTRALIA	
INTERNATIONAL DEFENCE INFORMATION CENTRES	
US Defense Technical Information Center	1
UK Dstl Knowledge Services	1
Canada Defence Research Directorate R&D Knowledge & Information Management (DRDKIM)	1
NZ Defence Information Centre	1
ABSTRACTING AND INFORMATION ORGANISATIONS	
Library, Chemical Abstracts Reference Service	1
Engineering Societies Library, US	1
Materials Information, Cambridge Scientific Abstracts, US	1
Documents Librarian, The Center for Research Libraries, US	1
INFORMATION EXCHANGE AGREEMENT PARTNERS	
National Aerospace Laboratory, Japan	1
National Aerospace Laboratory, Netherlands	1
SPARES	5 Printed

Total number of copies: 37 Printed: 14 PDF: 23

Page classification: UNCLASSIFIED

DEFENCE SCIENCE AND TECHNOLOGY ORGANISATION DOCUMENT CONTROL DATA	1. PRIVACY MARKING/CAVEAT (OF DOCUMENT)

2. TITLE	3. SECURITY CLASSIFICATION (FOR UNCLASSIFIED REPORTS THAT ARE LIMITED RELEASE USE (L) NEXT TO DOCUMENT CLASSIFICATION)
Environmental Durability Trial of Bonded Composite Repairs to Metallic Aircraft Structure	Document (U) Title (U) Abstract (U)
4. AUTHOR(S)	5. CORPORATE AUTHOR
Andrew Rider, Ian Williams Ed Shum and Leo Mirabella	Defence Science and Technology Organisation 506 Lorimer St Fishermans Bend Victoria 3207 Australia

6a. DSTO NUMBER	6b. AR NUMBER	6c. TYPE OF REPORT	7. DOCUMENT DATE
DSTO-TR-1685	AR-013-333	Technical Report	February 2005

8. FILE NUMBER	9. TASK NUMBER	10. TASK SPONSOR	11. NO. OF PAGES	12. NO. OF REFERENCES
2004/1094552	AIR 04/241	DGTA	50	17

13. URL on the World Wide Web	14. RELEASE AUTHORITY
http://www.dsto.defence.gov.au/corporate/reports/DSTO-TR-1685.pdf	Chief, Air Vehicles Division

15. SECONDARY RELEASE STATEMENT OF THIS DOCUMENT

Approved for public release

OVERSEAS ENQUIRIES OUTSIDE STATED LIMITATIONS SHOULD BE REFERRED THROUGH DOCUMENT EXCHANGE, PO BOX 1500, EDINBURGH, SA 5111

16. DELIBERATE ANNOUNCEMENT

No Limitations

17. CITATION IN OTHER DOCUMENTS Yes

18. DEFTEST DESCRIPTORS

adhesives, bond durability, environmental exposure, composite repairs

19. ABSTRACT

An agreement between DSTO and the US Air Force Research Laboratory (AFRL) was established as a part of a larger Aging Aircraft Project Agreement (PA). As a part of this agreement a large experimental program was organised to examine the long-term environmental durability of bonded composite repairs to metallic aircraft structure. An important aspect of the program was to examine the reliability and performance of current or recently developed surface treatments for metallic surfaces being repaired in field situations. The program involved the production of over 100 metal skinned honeycomb beam samples that were each patched with boron composite doublers. The beam samples are now being cyclically loaded in four point bending rigs at the DSTO tropical test facility in Innisfail, northern Queensland. It was anticipated that cyclic loading of the beams would result in adhesive disbonding for samples where the surface treatments were known to be inferior on the basis of accelerated laboratory testing. The overall results were hoped to enable the durability of metal to adhesive bonds present in boron composite repairs to be assessed for conditions similar to those expected in aircraft operating environments. An additional outcome of the research was hoped to be the ability to correlate accelerated durability testing conducted in the laboratory with more realistic aging conditions expected in aircraft service.

Page classification: UNCLASSIFIED